A new kentriodontid (Cetacea: Odontoceti) from the middle Miocene of the western North Pacific and a revision of kentriodontid phylogeny (#52427)

First submission

Guidance from your Editor

Please submit by **2 Nov 2020** for the benefit of the authors (and your $200 publishing discount) .

Structure and Criteria
Please read the 'Structure and Criteria' page for general guidance.

Custom checks
Make sure you include the custom checks shown below, in your review.

Raw data check
Review the raw data.

Image check
Check that figures and images have not been inappropriately manipulated.

Privacy reminder: If uploading an annotated PDF, remove identifiable information to remain anonymous.

Files

Download and review all files from the materials page.

12 Figure file(s)
1 Table file(s)
5 Other file(s)

Custom checks

New species checks

- Have you checked our new species policies?
- Do you agree that it is a new species?
- Is it correctly described e.g. meets ICZN standard?

Structure and Criteria

Structure your review

The review form is divided into 5 sections. Please consider these when composing your review:

1. **BASIC REPORTING**
2. **EXPERIMENTAL DESIGN**
3. **VALIDITY OF THE FINDINGS**
4. General comments
5. Confidential notes to the editor

You can also annotate this PDF and upload it as part of your review

When ready submit online.

Editorial Criteria

Use these criteria points to structure your review. The full detailed editorial criteria is on your guidance page.

BASIC REPORTING

- Clear, unambiguous, professional English language used throughout.
- Intro & background to show context. Literature well referenced & relevant.
- Structure conforms to PeerJ standards, discipline norm, or improved for clarity.
- Figures are relevant, high quality, well labelled & described.
- Raw data supplied (see PeerJ policy).

EXPERIMENTAL DESIGN

- Original primary research within Scope of the journal.
- Research question well defined, relevant & meaningful. It is stated how the research fills an identified knowledge gap.
- Rigorous investigation performed to a high technical & ethical standard.
- Methods described with sufficient detail & information to replicate.

VALIDITY OF THE FINDINGS

- Impact and novelty not assessed. Negative/inconclusive results accepted. *Meaningful* replication encouraged where rationale & benefit to literature is clearly stated.
- All underlying data have been provided; they are robust, statistically sound, & controlled.
- Speculation is welcome, but should be identified as such.
- Conclusions are well stated, linked to original research question & limited to supporting results.

Standout reviewing tips

The best reviewers use these techniques

Tip	*Example*
Support criticisms with evidence from the text or from other sources	*Smith et al (J of Methodology, 2005, V3, pp 123) have shown that the analysis you use in Lines 241-250 is not the most appropriate for this situation. Please explain why you used this method.*
Give specific suggestions on how to improve the manuscript	*Your introduction needs more detail. I suggest that you improve the description at lines 57- 86 to provide more justification for your study (specifically, you should expand upon the knowledge gap being filled).*
Comment on language and grammar issues	*The English language should be improved to ensure that an international audience can clearly understand your text. Some examples where the language could be improved include lines 23, 77, 121, 128 – the current phrasing makes comprehension difficult.*
Organize by importance of the issues, and number your points	*1. Your most important issue* *2. The next most important item* *3. …* *4. The least important points*
Please provide constructive criticism, and avoid personal opinions	*I thank you for providing the raw data, however your supplemental files need more descriptive metadata identifiers to be useful to future readers. Although your results are compelling, the data analysis should be improved in the following ways: AA, BB, CC*
Comment on strengths (as well as weaknesses) of the manuscript	*I commend the authors for their extensive data set, compiled over many years of detailed fieldwork. In addition, the manuscript is clearly written in professional, unambiguous language. If there is a weakness, it is in the statistical analysis (as I have noted above) which should be improved upon before Acceptance.*

A new kentriodontid (Cetacea: Odontoceti) from the middle Miocene of the western North Pacific and a revision of kentriodontid phylogeny

Zixuan Guo Corresp., Equal first author, [1], **Naoki Kohno** Equal first author, [1, 2]

[1] Faculty of Life and Environmental Sciences, University of Tsukuba, Tsukuba, Japan
[2] Department of Geology and Paleontology, National Museum of Nature and Science, Tsukuba, Japan

Corresponding Author: Zixuan Guo
Email address: guo_z@geol.tsukuba.ac.jp

A new species of an extinct dolphin belonging to the kentriodontids, i.e., *Kentriodon sugawarai*, sp. nov., is described from the lower Miocene Kadonosawa Formation in Ninohe City, Iwate Prefecture, northern Japan. The holotype of *Kentriodon sugawarai*, sp. nov., is consisted of a partial skull with ear bones, mandibular fragments, and some postcranial bones. The new species shares unique character with other species of the genus: the external auditory meatus is narrow. However, it differs from other species of the genus in having narrow width of the squamosal lateral to the exoccipital, dorsolateral edge of the internal opening of the infraorbital foramen is formed by the maxilla and the lacrimal or the jugal, and the anterior dorsal infraorbital foramina present three or more. Our phylogenetic analysis using an integrated data matrix from previous studies, based on 393 characters for 103 Odontoceti taxa, resulted in that the kentriodontids are a monophyletic group and recognized as a sister group to the crown Dephinoidea including the Delphinidae, Phocoenidae and Monodontidae. Our analysis also indicates that the dynamic renewal of the acoustic apparatus would have occurred in the Delphinoidea with the monophyletic Kentriodontidae during their evolution and diversification.

A new kentriodontid (Cetacea: Odontoceti) from the middle Miocene of the western North Pacific and a revision of kentriodontid phylogeny

Zixuan Guo[1], Naoki Kohno[1,2]

[1] Faculty of Life and Environmental Sciences, University of Tsukuba, Tsukuba, Japan
[2] Department of Geology and Paleontology, National Museum of Nature and Science, Tsukuba, Japan

Corresponding Author:
Zixuan Guo[1]
University of Tsukuba, 1-1-1 Tennodai, Tsukuba, 305-8577, Japan
Email address: guo_z@geol.tsukuba.ac.jp

Abstract

A new species of an extinct dolphin belonging to the kentriodontids, i.e., *Kentriodon sugawarai*, sp. nov., is described from the lower Miocene Kadonosawa Formation in Ninohe City, Iwate Prefecture, northern Japan. The holotype of *Kentriodon sugawarai*, sp. nov., ~~is consisted~~ of a partial skull with ear bones, mandibular fragments, and some postcranial bones. The new species shares unique character with other species of the genus: the external auditory meatus is narrow. However, it differs from other species of the genus in having narrow width of the squamosal lateral to the exoccipital, dorsolateral edge of the internal opening of the infraorbital foramen is formed by the maxilla and the lacrimal or the jugal, and the anterior dorsal infraorbital foramina ~~present~~ three ~~or more~~. Our phylogenetic analysis using an integrated data matrix from previous studies, based on 393 characters for 103 Odontoceti taxa, resulted in that the kentriodontids are a monophyletic group and recognized as a sister group to the crown Dephinoidea including the Delphinidae, Phocoenidae and Monodontidae. Our analysis also indicates that the dynamic renewal of the acoustic apparatus would have occurred in the Delphinoidea with the monophyletic Kentriodontidae during their evolution and diversification.

Introduction

The Dephinoidea has been thought to ~~be~~ emerge~~d~~ in the early Miocene (Gatesy et al., 2013) and are most diversified marine mammal~~s~~ in the world. However, their origin and adaptation are still in a puzzle. Proceeding in the emergence of the Dephinoidea, small coastal~~ly~~ odontocetes known as kentriodontids (Barnes & Mitchell, 1984; Barnes, 1985; Muizon, 1988a)~~,~~ showed high diversity during early to late Miocene (Ichishima et al., 1994). The group has been considered to be stem delphinoids based on their primitive morphologies and still had retained several ancestral characters of odontocetes as a whole (Barnes, 1978). For instance, asymmetric nasal and premaxillary bones have commonly been observed in the modern odontocetes, but the symmetrical condition~~s~~ of these bones ~~still have~~ retained in the kentriodontids. The interpretation for the evolutionary pattern of the Delphinoidea relies highly upon the process of morphological transformations in their stem group, while the relationships of such a stem group, the kentriodontids, have remained debated.

In the initial stage of the studies on ~~the~~ kentriodontids, they were considered to be a monophyletic family, the Kentriodontidae (e.g. Barnes, 1978; Barnes, 1985; Muizon, 1988a, 1988b; Ichishima et al., 1994). However, recent studies have advocated that the 'kentriodontids' are paraphyletic and are subdivided into several clades by different combination of taxa within the Delphinoidea as a broad sense (e.g. Lambert et al., 2017; Peredo, Uhen & Nelson, 2018; Kimura & Hasegawa, 2019). Because additional specimens of 'kentriodontids' have been accumulated, and molecular phylogeny of the cetaceans have recently established considerably (e.g. McGowen, Spaulding & Gatesy, 2009; McGowen et al., 2011; McGowen et al., 2020; Geisler et al., 2011), more comprehensive study for the phylogeny of this group is necessary. Recent studies have concentrated to investigate the phylogeny of this group (Lambert et al., 2017; Peredo, Uhen & Nelson, 2018; Kimura & Hasegawa, 2019) and show results that the kentriodontids may not be monophyletic but polyphyletic. Particularly, Peredo, Uhen & Nelson (2018) rectify the family Kentriodondae, ~~assert~~ only *Wimahl, Kampholophus* and *Kentriodon* ~~assigned to the family~~. However, some other phylogenetic studies (e.g. Murakami et al., 2014; Tanaka and Fordyce, 2014, 2016; Tanaka et al., 2017; Lambert et al., 2018) using different character set and data matri~~x~~ displayed some kentriodontid taxa with different topology. In other words, the relationship of the Delphinoidea is still in controversy.

Here, we describe a new species of the kentriodontid from the middle Miocene of Japan. The specimen includes a braincase of the skull with a well-preserved tympanoperiotics. We also reassess the phylogenetic relationships of the kentriodontids with molecular consensus and debate on the evolution of the Delphinoidea including the kentriodontids.

Materials & Methods

Nomenclatural acts

The electronic version of this article in Portable Document Format (PDF) will represent a published work according to the International Commission on Zoological Nomenclature (ICZN), and hence the new names contained in the electronic version are effectively published under that Code from the electronic edition alone. This published work and the nomenclatural acts it contains have been registered in ZooBank, the online registration system for the ICZN. The ZooBank LSIDs (Life Science Identifiers) can be resolved and the associated information viewed through any standard web browser by appending the LSID to the prefix http://zoobank.org/. The LSID for this publication is: urn:lsid:zoobank.org:pub:B0E9467F-CDD3-4AF4-83FE-40CE09D15700. The online version of this work is archived and available from the following digital repositories: PeerJ, PubMed Central and CLOCKSS

Anatomical terminology

We follow Mead & Fordyce (2009) for the terminology of skull and ear bone elements.

Phylogenetic Methods

The phylogenetic position of the new specimen being described here was analyzed based on the characters and the character matrix combined from Tanaka et al. (2017) and Lambert et al. (2017). The character list and the data matrix by Tanaka et al. (2017) was originally formalized by Geisler et al. (2011) and modified with additional characters by Murakami et al. (2012) to understand intraspecific relationships of the Phocoenidae within the crown Delphinoidea, and then it was re-modified by Tanaka & Fordyce (2014). The Tanaka et al. (2017) data matrix included 87 taxa and 284 characters, but this ~~data~~ matrix included ~~only~~ 3 taxa of kentriodontids: i.e., *Kentriodon pernix* Kellogg 1927, *Atocetus iquensis* Muizon 1988b and *Hadrodelphis calvertense* Dawson 1996. By contrast, the Lambert et al. (2017) data matrix was also based on Geisler, Godfrey & Lambert (2012), but they included 112 taxa and 324 characters with 12 taxa of kentriodontids: i.e., *Delphinodon dividum* True 1912, *Kentriodon pernix* Kellogg 1927, *Rudicetus squalodontoides* Bianucci 2001, *Hadrodelphis calvertense* Dawson 1996, *Kampholophus serrulus* Rensberger 1969, *Macrokentriodon morani* Dawson 1996, *Tagicetus joneti* Lambert, Estevens & Smith 2005, *Pithanodelphis cornutus* Abel 1905, *Atocetus nasalis* Muizon 1988a, *Atocetus iquensis* Muizon 1988b, *Lophocetus calvertensis* Cope 1867 and *Lophocetus repenningi* Barnes 1978. However, the character set used for their phylogenetic analysis was originally formularized for the taxa within much 'lower' clade of the Odontoceti (e.g., Geisler et al., 2011; Lambert et al., 2017; Peredo, Uhen & Nelson, 2018; Kimura & Hasegawa, 2019). Consequently, these two streams of studies on odontocete phylogeny including kentriodontids have not been comparative to each other, and the included taxa of kentriodontids and character combination to analyze their phylogenetic relationships were far different to each other, too. To resolve these problems, we performed a phylogenetic analysis based on the combined characters and kentriodontid taxa from previous studies such as Geisler, Godfrey & Lambert (2012), Murakami et al. (2012), Tanaka & Fordyce (2014), Tanaka et al. (2017), Lambert et al. (2017), Peredo, Uhen & Nelson (2018) and Kimura & Hasegawa (2019). The ~~resultant~~ data matrix of our study is based on 103 taxa including almost all the kentriodontids and 393 morphological characters (see Supplemental Information), with a tree constraint based on the molecular phylogenetics of the extant cetaceans by McGowen, Spaulding & Gatesy (2009), McGowen et al. (2011) and McGowen et al. (2020). In regard to the kentriodontids, we included the following 15 taxa of described kentriodontids into our data matrix (see also Supplemental Information): *Tagicetus joneti* Lambert, Estevens & Smith 2005 from the middle Miocene of Portugal (Lambert, Estevens & Smith, 2005), *Pithanodelphis cornutus* Abel 1905 from the upper Miocene of Belgiun (Flower, 1872), *Liolithax pappus* Barnes 1978 from the middle Miocene of USA (Barnes, 1978), *Atocetus nasalis* Muizon 1988b from the upper Miocene of USA (Muizon, 1988b), *Rudicetus squalodontoides* Bianucci 2001 from the lower to upper Miocene of Italy (Bianucci, 2001), *Kampholophus serrulus* Rensberger 1969 from the lower Miocene of USA (Rensberger, 1969), *Macrokentriodon morani* Dawson 1996 from the lower Miocene of USA (Dawson, 1996), *Lophocetus calvertensis* Cope 1867 from the upper Miocene of USA (Cope, 1867), *Lophocetus repenningi* Barnes 1978 from the middle Miocene of USA (Barnes, 1978), *Delphinodon dividum* True 1912 from the lower Miocene of USA (True, 1912), *Wimahl chinookensis* Peredo, Uhen & Nelson 2018 from the lower Miocene of USA (Peredo, Uhen & Nelson, 2018), *Kentriodon nakajimai* Kimura & Hasegawa 2019 from the middle to late Miocene of Japan (Kimura & Hasegawa, 2019), *Kentriodon diusinus* Salinas-Márquez et al. 2014 from the middle Miocene of USA (Salinas-Márquez et al., 2014), *Kentriodon schneideri* Whitmore & Kaltenbach 2008 from the middle Miocene of USA (Whitmore & Kaltenbach, 2008), *Kentriodon obscurus* Kellogg 1931 from the middle Miocene of USA (Kellogg, 1931).

Although more than half of the kentriodontid taxa had not been coded to complete our integrated data matrix to locate their phylogenetic positions, our observations and codings for the rest of taxa were in agreement with at least the coding traits for taxa already coded by previous studies. Therefore, it could be safe to code character states for the taxa of the above-mentioned kentriodontids that were not coded before based on our own observations and integrate all the codings into our new data matrix.

The phylogenetic analysis was performed with TNT 1.5 (Goloboff, Farris & Nixon, 2008; Goloboff & Catalano, 2016). All characters were treated as unweighted and unordered, using the "New Technology Search" tasked to find minimum length trees 1,000 times, under the tree constraint based on the molecular evidence from the extant taxa (McGowen, Spaulding & Gatesy, 2009; McGowen et al., 2011; McGowen et al., 2020).

SYSTEMATIC PALEONTOLOGY

CETACEA Brisson, 1762
ODONTOCETI Flower, 1867
DELPHINIDA Muizon, 1988a
KENTRIODONTIDAE Slijper, 1936

Emended Diagnosis of Family: Differing from other families in having the following derived characters: premaxillae are compressed mediolaterally at anterior of the rostrum (Chr. 3), the mesorostral groove constricted posteriorly, anterior to the nares and behind the level of the antorbital notch, then rapidly diverging anteriorly (Chr. 7), anterior edge of the supraorbital process is oriented anterolaterally, forms an angle between 35° and 60° (Chr. 50), the dorsolateral edge of internal opening of the infraorbital foramen is formed by the lacrimal or the jugal (Chr. 58), the infratemporal crest forms well-defined curved ridge on the posterior edge of sulcus for the optic nerve (Chr. 64), the premaxillary foramen is located medially (Chr. 72), the alisphenoid is broadly exposed laterally in the temporal fossa (Chr. 160), suture between both the palatines and both the maxillae is straight transversely or bowed anteriorly (Chr. 179), the external auditory meatus is wide (Chr. 225), angle formed by basioccipital crests as ca. 15–40° in ventral view (Chr. 229), the hypoglossal foramen is separated from the jugular foramen or the jugular notch by thick bone (Chr. 231), most convex part of the pars cochlearis is on the ventrolateral surface (Chr. 283).

Kentriodon Kellogg, 1927

Emended Diagnosis of Genus: The genus *Kentriodon* differing from other genera of the kentriodontids (incl. *'Kentriodon' diusinus*) by having narrow external auditory meatus (Chr. 225).

Kentriodon sugawarai, sp. nov.

LSID: urn:lsid:zoobank.org:act:0D209916-B472-44A7-B7AB-29682FA945C4

Holotype: NHFM-F 001, incomplete skull including the braincase, right tympanoperiotics, fragments of left and right mandibles, partial atlas, and one tooth, lacking most of the rostrum.
Diagnosis of Species: Differing from *K. schneideri* by the convex~~ed~~ occipital (Chr. 176). Differing from *K. pernix*, *K. nakajimai* and *K. obscurus* by the following characters: the dorsolateral edge of the internal opening of the infraorbital foramen is formed by the maxilla and the lacrimal or the jugal (Chr. 58), ~~the~~ anterior dorsal infraorbital foramina ~~present three or more~~ (Chr. 65), anterolateral corner of the nasal lacks a distinct process (Chr. 136), width of the squamosal lateral to the exoccipital is narrow (Chr. 170), anterior level of the pterygoid sinus fossa is interrupted posterior to, or the level of, the antorbital notch (Chr. 193) and the ventral edge of the anterior process of the periotic is clearly concave in lateral view (Chr. 245). Differing further from *K. nakajimai*, *K. diusinus* and *K. schneideri* by having deep emargination of posterior edge of zygomatic process by the neck muscle fossa. Differing from *K. hobetsu*, *K. schneideri* and *K. pernix* by having narrow exoccipital in width. Differing from *K. obscurus* and *K. pernix* by having the aperture for cochlear aqueduct smaller than the aperture for vestibular aqueduct. Differing further from *K. pernix* by having the shallow lateral furrow of the tympanic bulla.
Etymology: The species is named in honor of Mr. Kohei Sugawara, the director of the Ninohe Museum of History and Folklore, for his longstanding contributions to geology and paleontology as well as local history of Ninohe district, and in gratitude for his encouragement and assistance to both of us throughout this study.
Type Locality: The holotype was collected in 1940s from the place close to Mabechi River, Ninohe City, Iwate Prefecture, Japan. Approximate geographical coordinates: 40°31'N, 141°31'E; (Fig. 1).
Formation and Age: Although the precise locality of NHFM-F 001 is presently uncertain, and therefore, the exact horizon from which NHFM-F 001 was collected is not clear, the siltstone matrix adhering NHFM-F 001 has produced the diatom flora including *Denticulopsis praelauta* (Oishi et al., 1999). Accordingly, NHFM-F 001 came from the middle to upper Kadonosawa Formation, because the Shikonai Siltstone Member of th~~e F~~ormation is dominated by silt to very fine sandstone. The Shikonai Siltstone Member of the Kadonosawa Formation is widely distributed in Ninohe City, including the locality area of NHFM-F 001. The siltstone layers of the Shirikonai Siltstone Member of the Kadonozawa Formation have produced rich diatom flora, and these are identified as those of the *Denticulopsis praelauta* Zone (TuZino & Yanagisawa, 2017; Tuzino et al., 2018). The range in age of this zone spans between 16.3 and 15.9 Ma (Yanagisawa & Akiba, 1998). The main part of the Kadonosawa Formation has yielded abundant molluskan fossils (Chinzei, 1966), and ~~has been reported~~ a tooth of *Desmosrylus* (Oishi & Kawakami, 1984). ~~Further, b~~ased on ostracods (Irizuki & Matsubara, 1994) and benthic foraminifera ~~(~~Kamemaru, Matsubara & Irizuki~~,~~ 1995)~~,~~ suggested environment of the Shikonai Siltstone Member of the Kadonosawa Formation is sublittoral to bathyal in depth.

DESCRIPTION

Cranium

The cranium lacks most of the rostrum anterior to the antorbital notch (Fig. 2), and the left orbit and parts of the left squamosal are also missing ~~away~~. In ventral view, the choanae is cracked, not connected with the bony nares and depressed by secondary deformation (Fig. 3). In dorsal view, the nasal and the premaxilla are almost symmetrical at the sagittal plane, while the midline of the occipital condyle is slightly skewed to the right rather than the midline of the nasal and premaxilla. In posterior view, the right temporal fossa slightly faces dorsolaterally while the left temporal fossa faces laterally, the dorsal part of the cranium might fall left by secondary deformation. In lateral view, the temporal fossa is long anteroposteriorly and ~~deep~~ dorsoventrally. The vertex is low and flat, formed by the frontals and the nasals.

Premaxilla

Most of the rostral portion of premaxillae ~~are~~ broken away. Broken section is just anterior ~~at the portion anterior~~ to the antorbital notch. The premaxillary foramen is just posterior to the broken section, and ~~on~~ the same level ~~of~~ the antorbital notch. Anteromedial to the premaxillary foramen, the anteromedial sulcus and the prenarial triangle cannot be visible posterior to the broken section. The posteromedial sulcus of the premaxilla is absent. The lateral margin of each side of the premaxilla is also broken, and the posterolateral sulcus cannot be recognized, and only remaining a recognizable premaxillary surface on right side of the maxilla. Anterior to the bony nares, the premaxillae are thin and flat, the premaxillary sac fossa on the premaxilla is weekly depressed. In lateral view, premaxillae form a low angle of about 20° ~~along~~ the anteroposterior axis of the cranium (Fig. 4). The premaxillae are symmetrical~~,~~ the knob-like posterior end of the premaxilla contacts the anterolateral corner of the nasal at ~~the~~ level slightly lower ~~to~~ the vertex.

Maxilla

The left maxilla is broken laterally, but the right antorbital notch is preserved. The maxillary-palatine suture and the cross-section of the infraorbital foramen is observed in the broken section (Fig. 5). The maxilla is generally flat transversely at the antorbital region, and there is no indication of ~~the~~ maxillary crest. The lateral margin of the maxilla is flat ~~at~~ its orbital area, but it is slightly concave posteriorly to the orbital. There are three anterior and one posterior dorsal infraorbital foramina on the right maxilla (Fig. 2). The anterior-most one of these is located just beside the maxillary-premaxillary suture, anteromedial to the antorbital notch. ~~O~~ther ~~two~~ small anterior dorsal infraorbital foramina are located at the level of the premaxillary sac fossa. The posterior dorsal infraorbital foramen is the largest, and its opening is located on the ascending process at the level of the nasals. In transition plate, the maxilla rises towards ~~to~~ the vertex gently at the ascending process but sharply at the vertex. Although the vertex is low, the maxilla faces laterally just lateral to the nasal and makes a pair of deep fossae intently lateral by the nasal and anteriorly by the nuchal crest. The posterior and lateral margins of the right maxilla are semicircular, and the posteromedial margin ~~connects~~ the supraoccipital ~~posteriorly on the right maxilla~~. In lateral view, the maxilla overlaps ~~on~~ the frontal dorsally, and form a thin plate posteriorly from the supraorbital margin of the frontal. It gradually thickens anteriorly by the antorbital process. In ventral view, the right ventral infraorbital foramen is preserved, while the lateral edge of the left ventral infraorbital foramen is broken away. The sutures of the maxilla to other bones are not clear since the lacrimal and palatine do not show distinct sutures.

Palatine and Pterygoid

The posterior half of the palatine is preserved. The palatine-maxilla suture is visible from the anterior side through the transverse section (Fig. 5). The palatine connects to the maxilla dorsally and thinner than the maxilla. The left and right palatines are not separated medially at the level of the transverse section just anterior to the antorbital notch. The left side of the palatine-pterygoid is broken laterally, but the parasagittal section of the left infraorbital foramen is observed (Fig. 3). Since the palatine-maxilla suture is not clear in the parasagittal section, the ventromedial edge of the infraorbital foramen is uncertain.

The pterygoids are well~~-~~preserved. Both the lateral and ventral laminae of the pterygoid and the pterygoid hamulus are also well~~-~~preserved. The anterior most of the pterygoid is located slightly posterior to the level of the antorbital notch. The pterygoid sinus is covered by the pterygoid. The anterior edge of the pterygoid sinus is slightly extended anteriorly to the level of the antorbital notch. The palatal surface is flat and convex ventrally. The sagittal portion of the palatal surface is slightly separated posteriorly. The hamular crest of the pterygoid is present but blunt, and it ~~is~~ diverge~~d~~ posteriorly in ventral view. The pterygoid hamulus is short, and it tapers posterolaterally by the hamular crest. It locates the posterolateral most of the lateral and ventral laminae of the pterygoid, just posterior to the infratemporal crest of the frontal. The medial lamina forms the anterolateral wall of the internal nares. The posterior lamina overlaps the basioccipital crest. It forms the pharyngeal crest and covers the alisphenoid ventrally.

Vomer

The vomer is visible dorsally, but it is covered by the pterygoid ventrally. ~~In view,~~ from the anterior transverse section (Fig. 5), the premaxilla does not make a roof that covers the vomer dorsally. The mesorostal canal is opened widely as a U-shape groove, started from 11 mm anterior to the anterior edge of the ~~boney~~ nares. In ventral view, the vomer is covered by the pterygoid ventrally at the choanae, and it is posteriorly overhung beneath the basioccipital.

Mesethmoid

The ectethmoid appears on the nasal septum. The nasal septum is narrow transversely and straight dorsally. It is as high as the level of the nasal process of the premaxilla and connects with the nasals. Because of this, the cribriform plate and the mesethmoid cannot be distinguishable in dorsal view.

Nasal

The shape of the nasal is subtriangular, and its transverse width is ~~wider~~ than its anteroposterior length. The left and right nasals are symmetrical. The nasal is slightly wider than the widest part of the ~~boney~~ nares, and its anterior margin is slightly narrower than its posterior margin. The lateral margin contacts with the posterior end of the premaxilla anterolaterally and contact with the maxilla laterally. The nasals also contact with the frontals posteromedially. The dorsal surface of the nasal is flat, and it is only slightly concave anterolaterally. There is no indication of ~~the~~ internasal fossa and has only the shallow internasal suture medially. The internasal suture is almost situated on the midline of the cranium. In anterior view, the anterior border of the nasal is slightly retracted posteriorly by the ~~boney~~ nares.

Frontal

The frontal is only exposed at the vertex. In dorsal view, the frontal is separated from the maxilla by the nasal. The frontal is elliptical, and it connects anterolaterally the nasal and posteriorly the supraoccipital. The frontal at the vertex is slightly higher than the nasal, ~~and it becomes~~ the highest point of the cranium. In lateral view, the orbital fossa is slightly concave and low, in line with the edge of the posterior rostrum (Fig. 4). In ventral view, the preorbital process is thick anteriorly. While the anterior most of the frontal is broken, the frontal-lacrimal suture is not clear. The postorbital process, though the ventral apex is broken, is somewhat narrow and triangular at the base, its apex is directed posteroventrally or ventrally. Both the preorbital and postorbital lobes of the pterygoid sinus are shallow or absent. The frontal groove is deep medially, extant anteriorly to the level of the posterior most of the infraorbital foramen. The infratemporal crest is curved just anterior to the optic canal.

Lacrimojugal Complex

The left antorbital process is broken away, and the right antorbital process is also broken anteriorly and laterally, so the shape and the composition of the anterior most of the antorbital process is not clear. Although the lacrimal-maxilla suture and lacrimal-jugal suture are not clear in dorsal view, there may be a lacrimal-maxilla suture in anterior view at the broken section of the antorbital process. The lacrimal is thicker than the maxilla at the broken section of the antorbital process. The right jugal connects the lacrimal exactly at the posterior most of the antorbital notch. The main part of the jugal is broken away, but its base is narrow and only preserved as a short pedicle.

Squamosal

The right glenoid process of the squamosal is missing ~~away~~, while the anterior part of the left glenoid process is preserved as a short base, but it is also broken at the squamosal fossa. The glenoid process seems to be long because the postorbital process is relatively far from the base of the glenoid process. The squamosal fossa is incomplete anteriorly, but it is shallow and somehow longer anteroposteriorly, and it faces dorsally. The lateral margin of the fossa is visible in dorsal view. The mandibular fossa is not preserved, while the tympanosquamosal recess can be observed medially. The tympanosquamosal recess is flat and wide, and its ventral surface is wrinkled. The falciform process is not preserved well, and the retroarticular or postglenoid process is also not clear because of the insufficient preservation. The posttympanic or retrotympanic process cannot be distinct.

Supraoccipital

In dorsal view, the supraoccipital is large. The nuchal crest is trapezoidal in outline, while it is medially concave at the level of the temporal fossa. It expands laterally toward to the exoccipital. In posterior view, the supraoccipital is inclined anteriorly, and thus, it is low. The ~~supra~~occipital shield is concave anterodorsally and convex posteroventrally. Anteriorly, just posterior to the nuchal crest, the supraoccipital forms a fossa medially that the anterior most surface directs posteriorly. Posteriorly, the ~~supra~~occipital shield bulges medially (Fig. 6). This bulge has a suture with supraoccipital, and it is collapsed in the right margin, though it may be a result of deformation. The supraoccipital is fused with the exoccipital with an undefined suture. There is no indication of ~~the~~ external occipital crest.

Exoccipital

The exoccipital is wide. It extends laterally from the temporal crest. and it is fused with basioccipital ventrally. The temporal crest ~~is overhung~~ the exoccipital posterolaterally, ~~extant~~ nearly to the posterior most of the cranium ~~without~~ condyles. The occipital condyle is prominent, and the condylar neck is developed, while there is no indication of dorsal condyloid fossa. The foramen magnum is almost circular with only slightly ellipse that narrows mediolaterally. In ventral view, the jugular notch is deep and narrow. The paroccipital process is wide. The hypoglossal foramen is opened at the jugular notch. The paroccipital concavity is deep and wide, and it is separated from the jugular notch.

Basioccipital

The basioccipital is strongly concave laterally, and the basioccipital crests face ventromedially at their margins. The basioccipital basin ~~in between the basioccipital crests~~ is ~~board,~~ The basioccipital crest is transversely and anteriorly narrow and expands anteroposteriorly. It connects with the posterior lamina of the pterygoid. Its posterior margin is rounded. Medial to the crest, the ventral surface is flat. The muscular tubercle on the basioccipital basin is not developed.

Periotic

The right periotic is preserved (Figs. 7 and 8). In dorsal and ventral view, the apex of the anterior process is mediolaterally flattened. Its anteroventral and anterodorsal angles are respectively tapered and directed anteriorly, with same level by the anterior keel. The anteroposterior length of the anterior process is nearly the same as that of the pars cochlearis. The anterior incisure is deep, and it separates the anterior process from the pars cochlearis. In lateral view, the parabullary ridge is concave. There is a flat surface anterior to the fovea epitubaria, which is circular and 2 mm ~~in length~~, might be the anterior bullar facet but very shallow. The fovea epitubaria is broad, and it receives ~~but not fuses with~~ the accessory ossicle of the tympanic bulla. There is a fossa posteromedial to the accessory ossicle and anteromedial to the mallear fossa. It receives the tubercle of the malleus. The mallear fossa is rounded and faces ventrally rather than medially. The lateral tuberosity is bulbous laterally to the mallear fossa. The epitympanic hiatus is concave just posterior to the lateral tuberosity. The hiatus accommodates the facial canal posteromedially. The vestibular window is rounded and slightly larger than the facial canal.

The medial outline of the pars cochlearis is rounded and compressed dorsoventrally. The cochlear window opens on the posterior wall of the pars cochlearis. The aperture for the cochlear aqueduct opens dorsally and is located close to the vestibular aqueduct ~~with~~ the same transverse level as the medial edge of the internal acoustic meatus. The aperture for the vestibular aqueduct is two times larger than the aperture for the cochlear aqueduct and located slightly posteriorly to the aperture for the cochlear aqueduct at the anteroposterior level. The internal acoustic meatus is large and funnel-like, with an anterolateral–posteromedial axis. The anterior most of the internal acoustic meatus is continued with the anterior incisure. The foramen singulare is located closer to the proximal opening of the facial canal rather than the spiral cribiform tract, separated by partitions from the proximal opening of the facial canal and the spiral cribiform tract. The proximal opening of the facial canal is slightly anteriorly to the spiral cribriform tract. The area cribrosa media ~~have~~ almost the same size ~~with~~ the spiral cribriform tract. The posterior process is short anteroventrally, while its posterior edge is directed ventrally. In lateral view, the posterior process forms a blunt right angle at the dorsoventral most. The posterior bullar facet is smooth and faces anteroventrally.

Tympanic bulla

The right tympanic bulla only lacks the anterodorsal crest, the sigmoid process and the posterior process (Figs. 9 and 10). The accessory ossicle is preserved but disarticulated with the tympanic bulla. The tympanic bulla is narrow and long, and its ventral margin is slightly concave in lateral view. The lateral furrow is absent or very shallow. The disarticulated accessory ossicle is rounded and moderate in size. It occupies the fovea epitubaria of the periotic. In ventral view, there is an antero-posterior liner fracture surface on the accessory ossicle. The involucrum tapers anteriorly, and the anterior spine is absent or very short. The dorsal and ventral margins of the involucrum are parallel and the dorsal margin is excavated just anterior to the posterior process. The ventromedial keel on the involucrum is unclear. The interprominential notch is shallow and continues to the median furrow. The median furrow is shallow. It widens anteriorly and direct laterally. The sigmoid process is large and rounded, and it fully covers the conical process in dorsal view. The posterior edge of the sigmoid process is thick. The conical process is dorsally high. The inner and outer posterior prominences extend posteriorly ~~as~~ same level, and they are almost equal in size. The posterior process, which is broken at its base, is rounded and thick. The facet for the posterior process of the periotic is smooth. The elliptical foramen can be observed between the outer and inner posterior pedicles.

Malleus

The malleus is isolated from the periotic (Fig. 11 A–F). The head is high anteromedially. The ventral margin of the tubercle is concave~~d~~. The manubrium of malleus forms a hook-like process at the medial margin, which directs anteriorly. The insertion for the tendon of the m. tensor tympani opens ventrally. The processus muscularis is small.

Mandible

Both left and right mandibles are preserved (Fig. 11 K–N), but the right mandible only preserves its posterior part, while the left mandible preserves its posteroventral part including the angular process and the ventral half of the mandibular condyle. Both mandibles are flat and thin, the mandibular foramen is shallow mediolaterally. ~~In~~ left mandible, the mylohyoid groove is shallow anterior to the angular process. It preserves a crest ventrally to the mylohyoid groove, while the mandibular canal is not started at the anterior most of the fragment. The posterior margin of the angular process is rounded, and ~~it concaves on~~ the buccal surface. The mandibular condyle is located more posteriorly than the angular process and has an anteriorly inward, deep, rounded curve between the angular process and the mandibular condyle. The condyle is concave on the buccal surface. The apex of the condyle ~~is faced~~ dorsomedially. The condylar articular surface is not preserved.

Tooth

One isolated tooth is preserved (Fig. 11 G–J). It is small and conical, at least 27 mm ~~in length~~ and 6.3 mm in maximum diameter at the portion of the root. The surface of the crown is smooth, and its apex is hooked. The tooth root is also smooth and conical, and it is 1.5 times longer than the crown. The cementum of the root is just slightly thicker than the crown, ~~and the proximal end of the tooth root also slightly turn to right angle to the deflection of the distal end~~.

Vertebra

~~A~~ fragment of the atlas is ~~only the vertebra~~ (Fig. 11 O, P). The ventral part of the ~~arc~~ without transverse process is preserved. In posterior view, the posterior articular surface is not well preserved, but it ~~is at least~~ not fused with the axis. In dorsal view, the anterior tubercle is short anteroposteriorly and relatively high ventrally. It ~~also has~~ a V-shape crest on its anterior surface~~.~~ ~~It starts~~ from the ventral most of the anterior articular facet to the ventral most of the anterior tubercle. The anterior articular facet is concave ventrally, and thin at the middle part.

Results of Phylogenetic Analyses

Our phylogenetic analyses found 256 most parsimonious trees with 3424 steps in total branch length. Each tree has a consistency index of 0.197 and a retention index of 0.564. The 50%

majority rule consensus of those trees is shown in Figure 12. The strict consensus tree is also shown in the Supplemental Information. The majority rule consensus tree shows that all the species previously identified as kentriodontids ~~were~~ nested in the monophyletic clade and positioned as the sister group to the crown Delphinoidea (i.e., ~~Delphiidae,~~ Phocoenidae and Monodontidae), and therefore, The kentriodontids were not ancestral to the crown delphinoids. The monophyly of the Kentriodontidae was supported by 14 synapomorphies as follows: premaxillae are compressed mediolaterally at anterior of the rostrum (Chr. 3), the mesorostral groove constricted posteriorly, anterior to the nares and behind the level of the antorbital notch, then rapidly diverging anteriorly (Chr. 7), anterior edge of the supraorbital process is oriented anterolaterally, ~~forms~~ an angle between 35° and 60° (Chr. 50), the dorsolateral edge of internal opening of the infraorbital foramen is formed by the lacrimal or the jugal (Chr. 58), the infratemporal crest forms well-defined curved ridge on the posterior edge of sulcus for the optic nerve (Chr. 64), the premaxillary foramen is located medially (Chr. 72), the alisphenoid is broadly exposed laterally in the temporal fossa (Chr. 160), suture between ~~both~~ the palatines and ~~both~~ the maxillae is straight transversely or bowed anteriorly (Chr. 179), the external auditory meatus is wide (Chr. 225), angle formed by basioccipital crests ~~as~~ ca. 15–40° in ventral view (Chr. 229), the hypoglossal foramen is separated from the jugular foramen or the jugular notch by thick bone (Chr. 231), most convex part of the pars cochlearis is on the ventrolateral surface (Chr. 283), the basihyal and the thyrohyal are fused (Chr. 332) and the lateral edge of transverse processes of lumbar vertebrae angled anteromedially 45° or more, relative to a parasagittal plane (Chr. 334). However, last two characters (i.e., Chrs. 332 and 334) are not ~~preserved on~~ most kentriodontid taxa.

Among the monophyletic Delphinoidea, NHFM-F 001 was nested in the kentriodontid clade and recognized as a sister taxon of *K. pernix, K. nakajimai* and *K. obscurus* (Fig. 12). In addition, ~~the monophyly of~~ *K. schneideri,* NHFM-F 001, *K. pernix, K. nakajimai* and *K. obscurus*, ~~except for~~ *K. diusinus,* was ~~recognized.~~ Thus, NHFM-F 001 is considered as belonging in the genus *Kentriodon*. However, NHFM-F 001 has quite a few autapomorphic characters among other *Kentriodon* species, and accordingly, a formal definition for NHFM-F 001 as a new species of the genus *Knetriodon* is warranted. Thus, we propose a new species within the genus, i.e., *Kentriodon sugawarai*, sp. nov.

Discussion and Conclusions

Phylogenetic Position of the Kentriodontids

The result of our phylogenetic analysis is apparently similar with that of Tanaka et al. (2017), but the interrelationship of the Delphinida (Inioidea + our concept of Kentriodontidae + crown Delphinoidea) is different from their result. In the Delphinida, the interrelationship of the crown Delphinoidea (Delphinidae + Monodontidae + Phocoenidae) is also similar with Tanaka et al. (2017), but the sister group relationships among the Delphinida (Inioidea + our Kentriodontidae) are different. Tanaka et al. (2017) included only three kentriodontids and suggested that they ~~were~~ paraphyletic. These three kentriodontids were located at the basal position for the crown

Delphinoidea. In recent studies on the relationships of the delphinidans, Lambert et al. (2017) and Peredo, Uhen & Nelson (2018) advocated that the ‘kentriodontids’ were ~~also considered to be paraphyletic~~, and these studies subdivided the so called ‘kentriodontids' into ~~5~~ paraphyletic or polyphyletic groups. Particularly, there unconstrained analysis suggested that the Lipotidae was recognized as a sister group to the paraphyletic ‘kentriodontid’ species, i.e., *Liolithax*, meaning that it was more closely related to some ‘kentriodontids' than Iniidae + Pontoporiidae, which was also different from the results of the molecular phylogen~~etics~~ (e.g., McGowen, Spaulding & Gatesy, 2009; McGowen et al., 2011; McGowen et al., 2020).

By contrast, our analysis suggest~~ed~~ ~~the monophyletic grouping of~~ all the species of the kentriodontids as discussed above. Although the monophyly of the kentriodontids has been proposed ~~by~~ some early studies (e.g., Barnes, 1978, 1985; Muizon, 1988a), intergeneric and specific relationships among the family are both different from our result. Our result suggests that ~~the~~ kentriodontids are divided into two monophyletic subgroups (fig. 12). One subgroup includes *Kampholophus*, *Wimahl*, *Rudicetus* and *Kentriodon*, while the other subgroup includes *Delphinodon, Tagicetus, Macrokentriodon, Liolithax, Hadrodelphis, Pithanodelphis, Lophocetus*, and *Atocetus*. The diagram shows agreements with Peredo, Uhen & Nelson (2018) and Kimura & Hsagawa (2019) at least in the former subgroup. On the other hand, they have suggested the taxa in the latter subgroup ~~that are divided~~ into four polyphyletic subgroups.

As mentioned above, we adopted our phylogenetic analysis with a tree constraint based on the molecular evidence by McGowen, Spaulding & Gatesy (2009), McGowen et al. (2011) and McGowen et al. (2020) as was also the case for Tanaka et al. (2017). Lambert et al. (2017) performed their phylogenetic analyses both with a tree constraint based on the molecular evidence and without such a tree constraint, and they preferred their unconstrained tree as a result from their multiple analyses. The study by Lambert et al. (2017) was so comprehensive that it might be the reason why the molecular evidence had not been used in later studies on the phylogeny of the Delphinida including the kentriodontids (e.g., Peredo, Uhen & Nelson, 2018; Kimura & ~~Hsagawa,~~ 2019, 2020). The molecular phylogenetics is now widely accepted to reconstruct the phylogenetic relationships of organisms, but its results are sometimes or often different from morphological data. Although those studies mentioned above chose the total evidence approach (parsimony analysis based both on molecular and morphological evidence) for their analyses, the resultant relationships they suggested are different from that of the analyses by molecular only (McGowen, Spaulding & Gatesy, 2009; McGowen et al., 2011; McGowen et al., 2020; Geisler et al., 2011; Lambert et al., 2020).

Interestingly, the phylogenetic relationships of the basal taxa within the Odontoceti as are suggested by some previous researches (e.g., Tanaka and Fordyce, 2016; Tanaka et al., 2017) are little different from our result. Particularly, the topology of our diagram shows that the clade including *Waipatia*, *Otekaikea* and *Awamokoa* is located more basal within the Odontoceti than previously thought. ~~It may also be the potential effect that t~~hese differences may occurred ~~since our integrated characters that are focused~~ on the relationships of the Delphinida like Tanaka & Fordyce (2016) and Tanaka et al. (2017) rather than focusing on more basal taxa within the

Odontoceti like Geisler et al. (2011). In this regard, the characters incorporated from Lambert et al. (2017) and Tanaka et al. (2017) could be better to resolve the relationships of both earlier and later diverging taxa of dolphins in the Delphinida within the Odontoceti.

Potentially Independent Diversifications of Kentriodontids Based on Ear Bones

At the time of the evolution and diversification of ~~the~~ delphinidans including the monophyletic kentriodontids, seven out of 18 synapomorphies are considered to be evolutionary changes of periotic and tympanic bulla features. These changes could be interpreted to be the result of their evolutionary innovation such as the potential specialization of their echolocation abilities among ~~the~~ odontocetes (Gutstein et al., 2014; Churchill et al., 2016). ~~Such~~ characters are the following: the processus muscularis of the malleus is sub-equal or longer than the manubrium (Chr. 237), the articulation of the anterior process with the squamosal is absent (Chr. 253), the anterior bullar facet is absent (Chr. 254), the dorsal surface of the periotic is nearly flat (Chr. 260), the foramen singulare is in common recess with the spiral cribiform tract, the transverse crest that separates it from the proximal opening of the facial nerve canal is low, and the proximal opening of the facial nerve canal within the internal acoustic ~~meatu~~ (Chr. 269), the aperture for the cochlear aqueduct is smaller than the aperture for the vestibular aqueduct (Chr. 272) and the dorsal margin of the involucrum of the tympanic bulla is excavated just anterior to the posterior process (Chr. 317). Also, the node uniting the kentriodontids and the crown delphinoids is highlighted by ~~additional~~ six auditory characters out of 11 synapomorphies ~~for the node~~: the apex of the anterior process of the periotic is thickened by the prominent dorsal tubercle giving ~~its~~ apex rectangular section on the plane of its body (Chr. 239), the contact of the anterior process of the petrosal with a portion of the ectotympanic bulla anterior to the accessory ossicle is absent (Chr. 249), the periotic articulates with squamosal along hiatus epitympanicus and adjacent regions on the posterior process (Chr. 286), mastoid exposure of the posterior process of the periotic on outside of skull is exposed externally (Chr. 292), lateral furrow of the tympanic bulla present a shallow groove (Chr. 303) and the ventral margin of the tympanic bulla in lateral view is concave (Chr. 307). Compared with other odontocetes, the ear bones of ~~the~~ delphinidans are highly specialized ~~rather than other groups~~ (e.g. Fraser & Purves, 1960; Gutstein et al., 2014), and the ear bones of ~~the~~ kentriodontids are much similar to the crown delphinoids rather than ~~the~~ inioids (see also Gutstein et al., 2014). These peculiarities of the periotic and tympanic bulla of the delphinidans are thought to have been emphasized by their diversification or specialization of functional relationships ~~among~~ the periotic, tympanic bulla and ~~related~~ portion of the skull during the process of the acquisition of much higher frequency (i.e., ultrasonic) sound hearing abilities (e.g. Cranford, Krysl & Amundin, 2010; Gutstein et al., 2014; Ary, 2017). It will also be related to the inner cochlear features and hearing capabilities like high-frequency sound hearing. These changes might also have given chance to diversify their abilities of echolocation (e.g. Churchill et al., 2016; Mourlam & Orliac, 2017; Costeur et al., 2018). In this regard, the kentriodontids was an independent group not so as a stem group to the crown delphinoids within the delphinidans, and they were a unique group by the diversification of their hearing abilities within the odontocetes. Specializations of hearing apparatus in the kentriodontids probably resulted in their high diversification during the period between the late early and early late Miocene, which might have been similar to the later diversification of the crown delphinoids after late Miocene.

Institutional abbreviations

NHFM-F Fossil collections of the Ninohe Museum of History and Folklore, Ninohe City, Iwate, Japan.

NMNS-PV Fossil vertebrate collections at the National Museum of Nature and Science, Tsukuba, Japan.

NSMT-M Marine mammal collections at the National Museum of Nature and Science, Tsukuba, Japan.

Acknowledgements

We wish to thank K. Sugawara (NMHF) and Y. Inaba (NMHF) for permitting us to describe NHFM-F 001. We also thank Y. Tajima (NMNS), T. Kimura (GMNH) for providing access to the collections under their care. Our thanks also go to Y. Tajima and T.K. Yamada (NMNS) and Y. Yanagisawa (Geological Survey of Japan) for providing useful discussion and advice. We appreciate K. Sashida (then University of Tsukuba, now Mahidol Univ.) and S. Agematsu (Univ. Tsukuba) for their help during field works. We are grateful to K. Sashida, S. Agematsu, K. Tanaka (Univ. Tsukuba), and Yasunari Shigeta (NMNS/Univ. Tsukuba) for their useful advice, discussion and generous encouragement during the course of this study.

References

Ary WJ. 2017. Form, function and phylogeny in the cetacean ear complex. San Diego State University, *ProQuest Dissertations Publishing* 10689605.

Barnes LG. 1978. A review of *Lophocetus* and *Liolithax* and their relationships to the delphinoid family Kentriodontidae (Cetacea: Odontoceti). *Bulletin of the Natural History Museum of Los Angeles County* 28:1–35.

Barnes LG. 1985. The Late Miocene dolphin *Pithanodelphis* Abel, 1905 (Cetacea-Kentriodontidae) from California.pdf. *Contributions in Science*:1–27.

Barnes LG, Mitchell ED. 1984. *Kentriodon obscurus* (Kellogg, 1931), a fossil dolphin (Mammalia: Kentriodontidae) from the Miocene Sharktooth Hill Bonebed in California. *Contributions in Science (Los Angeles)* 353:1–23.

Bianucci G. 2001. A new genus of kentriodontid (cetacea: Odontoceti) from the miocene of South Italy. *Journal of Vertebrate Paleontology* 21:573–577. DOI: 10.1671/0272-4634(2001)021[0573:ANGOKC]2.0.CO;2.

Chinzei K. 1966. Younger Tertiary geology of the Mabechi River valley, northeast Honshu, Japan. *Journal of the Faculty of Science, the University of Tokyo. Sect. II* 16:161–208.

Churchill M, Martinez-Caceres M, de Muizon C, Mnieckowski J, Geisler JH. 2016. The Origin of High-Frequency Hearing in Whales. *Current Biology* 26:2144–2149. DOI: 10.1016/j.cub.2016.06.004.

Cope ED. 1867. An Addition to the Vertebrate fauna of the Miocene Period, with a Synopsis of the Extinct Cetacea of the United States. *Proceedings of the Academy of Natural Sciences of Philidelphia* 19:138–156.

Costeur L, Grohé C, Aguirre-Fernández G, Ekdale E, Schulz G, Müller B, Mennecart B. 2018. The bony labyrinth of toothed whales reflects both phylogeny and habitat preferences. *Scientific Reports* 8. DOI: 10.1038/s41598-018-26094-0.

Cranford TW, Krysl P, Amundin M. 2010. A new acoustic portal into the odontocete ear and vibrational analysis of the tympanoperiotic complex. *PLoS ONE* 5. DOI: 10.1371/journal.pone.0011927.

Dawson SD. 1996. A new kentriodontid dolphin (cetacea; delphinoidea) from the middle miocene choptank formation, Maryland. *Journal of Vertebrate Paleontology* 16:135–140. DOI: 10.1080/02724634.1996.10011291.

Flower WH. 1872. On the recent Ziphioid whales, with a Description of the Skeleton of *Berardius arnouxi*. *The Transactions of the Zoological Society of London* 8:203–234. DOI: 10.1111/j.1469-7998.1872.tb08572.x.

Fraser FC, Purves PE. 1960. Hearing in Cetaceans. Evolution of the accessory air sacs and the structure and function of the outer and middle ear in recent cetaceans. *Bulletin of the British Museum (Natural History) Zoology* 7:1–140, 53 pls. frontis.

Gatesy J, Geisler JH, Chang J, Buell C, Berta A, Meredith RW, Springer MS, McGowen MR. 2013. A phylogenetic blueprint for a modern whale. *Molecular Phylogenetics and Evolution* 66:479–506. DOI: 10.1016/j.ympev.2012.10.012.

Geisler JH, Godfrey SJ, Lambert O. 2012. A new genus and species of late Miocene inioid (Cetacea, Odontoceti) from the Meherrin River, North Carolina, U.S.A. *Journal of Vertebrate Paleontology* 32:198–211. DOI: 10.1080/02724634.2012.629016.

Geisler JH, McGowen MR, Yang G, Gatesy J. 2011. A supermatrix analysis of genomic, morphological, and paleontological data from crown Cetacea. *BMC Evolutionary Biology* 11. DOI: 10.1186/1471-2148-11-112.

Goloboff PA, Catalano SA. 2016. TNT version 1.5, including a full implementation of phylogenetic morphometrics. *Cladistics* 32:221-238. DOI: 10.1111/cla.12160

Goloboff PA, Farris JS, Nixon KC. 2008. TNT, a free program for phylogenetic analysis. *Cladistics* 24:774–786. DOI: 10.1111/j.1096-0031.2008.00217.x.

Gutstein CS, Figueroa-Bravo CP, Pyenson ND, Yury-Yañez RE, Cozzuol MA, Canals M. 2014. High frequency echolocation, ear morphology, and the marine-freshwater transition: A comparative study of extant and extinct toothed whales. *Palaeogeography, Palaeoclimatology, Palaeoecology* 400:62–74. DOI: 10.1016/j.palaeo.2014.01.026.

Ichishima H, Barnes LG, Fordyce RE, Kimura M, Bohaska DJ. 1994. A review of kentriodontine dolphins (Cetacea; Deiphinoidea; Kentriodontidae): Systematics and biogeography. *Island Arc* 3:486–492. DOI: 10.1111/j.1440-1738.1994.tb00127.x.
Irizuki T, Matsubara T. 1994. Vertical changes of depositional environments of the Lower to Middle Miocene Kadonosawa Formation based on analyses of fossil ostracode faunas. *The Journal of the Geological Society of Japan* 100:136–149. [Japanese with English abstract]
Kamemaru A, Matsubara T, and Irizuki T. 1995. Foraminiferal assemblage in the Lower to Middle Miocene Kadonosawa Formation at the type locality, Iwate Prefecture. *Abstract of the 102nd Annual Meeting of the Geological Society of Japan*:93. [Japanese]
Kellogg R. 1931. Pelagic Mammals from the Temblor Formation of the Kern River Region, California. *Proceedings of the California Academy of Sciences* XIX:217–397.
Kimura T, Hasegawa Y. 2019. A new species of *Kentriodon* (Cetacea, Odontoceti, Kentriodontidae) from the Miocene of Japan. *Journal of Vertebrate Paleontology* 39:1–14. DOI: 10.1080/02724634.2019.1566739.
Kimura T, Hasegawa Y. 2020. *Norisdelphis annakaensis*, A new Miocene delphinid from Japan. *Journal of Vertebrate Paleontology*:e1762628. DOI: 10.1080/02724634.2020.1762628.
Lambert O, Bianucci G, Urbina M, Geisler JH. 2017. A new inioid (Cetacea, Odontoceti, Delphinida) from the Miocene of Peru and the origin of modern dolphin and porpoise families. *Zoological Journal of the Linnean Society* 179:919–946. DOI: 10.1111/zoj.12479.
Lambert O, Collareta A, Benites-Palomino A, Di Celma C, de Muizon C, Urbina M, Bianucci G. 2020. A new small, mesorostrine inioid (Cetacea, Odontoceti, Delphinida) from four upper Miocene localities in the Pisco Basin, Peru. *Papers in Palaeontology*:spp2.1332. DOI: 10.1002/spp2.1332.
Lambert O, Estevens M, Smith R. 2005. A new kentriodontine dolphin from the middle Miocene of Portugal. *Acta Palaeontologica Polonica* 50:239–248.
Lambert O, Muizon C de, Malinverno E, Di Celma C, Urbina M, Bianucci G. 2018. A new odontocete (toothed cetacean) from the Early Miocene of Peru expands the morphological disparity of extinct heterodont dolphins. *Journal of Systematic Palaeontology* 16:981–1016. DOI: 10.1080/14772019.2017.1359689.
McGowen MR, Montgomery SH, Clark C, Gatesy J. 2011. Phylogeny and adaptive evolution of the brain-development gene microcephalin (MCPH1) in cetaceans. *BMC Evolutionary Biology* 11. DOI: 10.1186/1471-2148-11-98.
McGowen MR, Spaulding M, Gatesy J. 2009. Divergence date estimation and a comprehensive molecular tree of extant cetaceans. *Molecular Phylogenetics and Evolution* 53:891–906. DOI: 10.1016/j.ympev.2009.08.018.
McGowen MR, Tsagkogeorga G, Álvarez-Carretero S, Dos Reis M, Struebig M, Deaville R, Jepson PD, Jarman S, Polanowski A, Morin PA, Rossiter SJ. 2020. Phylogenomic Resolution of the Cetacean Tree of Life Using Target Sequence Capture. *Systematic Biology* 69:479–501. DOI: 10.1093/sysbio/syz068.

Mead JG, Fordyce RE. 2009. The therian skull: a lexicon with emphasis on the odontocetes. *Smithsonian Contributions to Zoology*:1–249. DOI: 10.5479/si.00810282.627.

Mourlam MJ, Orliac MJ. 2017. Infrasonic and Ultrasonic Hearing Evolved after the Emergence of Modern Whales. *Current Biology* 27:1776-1781.e9. DOI: 10.1016/j.cub.2017.04.061.

Muizon C de. 1988a. Les relations phylogénétiques des Delphinida (Cetacea, Mammalia). *Annales de Paléontologie* 74:159–227.

Muizon C de. 1988b. Les vertébrés fossiles de la Formation Pisco (Pérou). Troisième partie: Les Odontocètes (Cetacea, Mammalia) du Miocène. *Travaux de l'Institut Français d'Etudes Andines* 78:1–244.

Murakami M, Shimada C, Hikida Y, Hirano H. 2012. Two new extinct basal phocoenids (Cetacea, Odontoceti, Delphinoidea), from the upper Miocene Koetoi Formation of Japan and their phylogenetic significance. *Journal of Vertebrate Paleontology* 32:1172–1185. DOI: 10.1080/02724634.2012.694337.

Murakami M, Shimada C, Hikida Y, Hirano H. 2014. Asymmetrical Basal Delphinoid Skull from the Upper Lower Miocene Yamato Formation of Hokkaido, Northern Japan: Implications on Evolution Of Cranial Asymmetry and Symmetry in Odontoceti. *Paleontological Research* 18:134–149. DOI: 10.2517/2014pr013.

Oishi M, Hasegawa Y, Yanagisawa Y, Matsubara T, Kikuchi H, Komori K, Kawamorita H. 1999. Miocene kentriodontid dolphins from Ninohe and Ichinohe, Iwate Prefecture, Japan. *Abstract of the 1999 Annual Meeting of the Palaeontological Society of Japan*:55. (January 29 - 31, 1999 at Sendai, Japan, Palaeontological Society of Japan). [Japanese]

Oishi M, Kawakami T. 1984. A new occurrence of desmostylian molar from the Miocene Kadonosawa Formation, Nisatai, Ninohe-City, Iwate Prefecture. *The Journal of the Geological Society of Japan* 90(1):55–58. [Japanese]

Peredo CM, Uhen MD, Nelson MD. 2018. A new kentriodontid (Cetacea: Odontoceti) from the early Miocene Astoria Formation and a revision of the stem delphinidan family Kentriodontidae. *Journal of Vertebrate Paleontology* 38. DOI: 10.1080/02724634.2017.1411357.

Rensberger JM. 1969. A new iniid cetacean from the Miocene of California. *University of California publications in geological sciences* 82:43.

Salinas-Márquez FM, Barnes LG, Flores-Trujillo JG, Aranda-Manteca FJ. 2014. A species of fossil dolphin (Cetacea; Delphinoidea; Kentriodontoidae) from the Middle Miocene of Baja California. *Boletin de la Sociedad Geologica Mexicana* 66:145–164. DOI: 10.18268/BSGM2014v66n1a11.

Tanaka Y, Abella J, Aguirre-Fernández G, Gregori M, Fordyce RE. 2017. A new tropical Oligocene dolphin from Montañita/Olón, Santa Elena, Ecuador. *PLoS ONE* 12:e0188380. DOI: 10.1371/journal.pone.0188380.

Tanaka Y, Fordyce RE. 2014. Fossil dolphin *Otekaikea marplesi* (Latest Oligocene, New Zealand) expands the morphological and taxonomic diversity of oligocene cetaceans. *PLoS ONE* 9. DOI: 10.1371/journal.pone.0107972.

Tanaka Y, Fordyce RE. 2016. Papahu-like fossil dolphin from Kaikoura, New Zealand, helps to fill the Early Miocene gap in the history of Odontoceti. *New Zealand Journal of Geology and Geophysics* 59:551–567. DOI: 10.1080/00288306.2016.1211540.

True FW. 1912. Description of a new fossil porpoise of the genus *Delphinodon* from the Miocene Formation of Maryland. *Journal of the Academy of Natural Sciences of Philadelphia* 2:165–197.

Tuzino T, Kudo T, Nakae S, Kondo R, Nishioka Y, Ueki T. 2018. *Geology of the Ichinohe district*. Quadrangle Series, 1:50,000, Geological Survey of Japan, AIST, 161p. [Japanese with English abstract]

TuZino T, Yanagisawa Y. 2017. Diatom occurence from the Miocene in the Ichinohe district, nothern part of Iwate Prefecture, NE Japan. *Bulletin of the Geological Survey of Japan* 68:237–258. [Japanese with English abstract]

Whitmore FC, Kaltenbach JA. 2008. Neogene Cetacea of the Lee Creek Phosphate Mine, North Carolina. *Virginia Museum of Natural History Special Publication* 14:181–269.

Yanagisawa Y, Akiba F. 1998. Refined Neogene diatom biostratigraphy for the northwest Pacific around Japan, with an introduction of code numbers for selected diatom biohorizons. *The Journal of the Geological Society of Japan* 104:395–414. DOI: 10.5575/geosoc.104.395.

Figure 1

Geographic and geologic context of *Kentriodon sugawarai* localities.

(A) the type locality of *Kentriodon sugawarai,* sp. nov., holotype, NHFM-F 001. (B) left, diatom zone and stratigraphic diagram, modified from Tuzino & Yanagisawa (2017). right, stratigraphic column of the Mabechi River, Ninohe City, Iwate Prefecture, Japan.

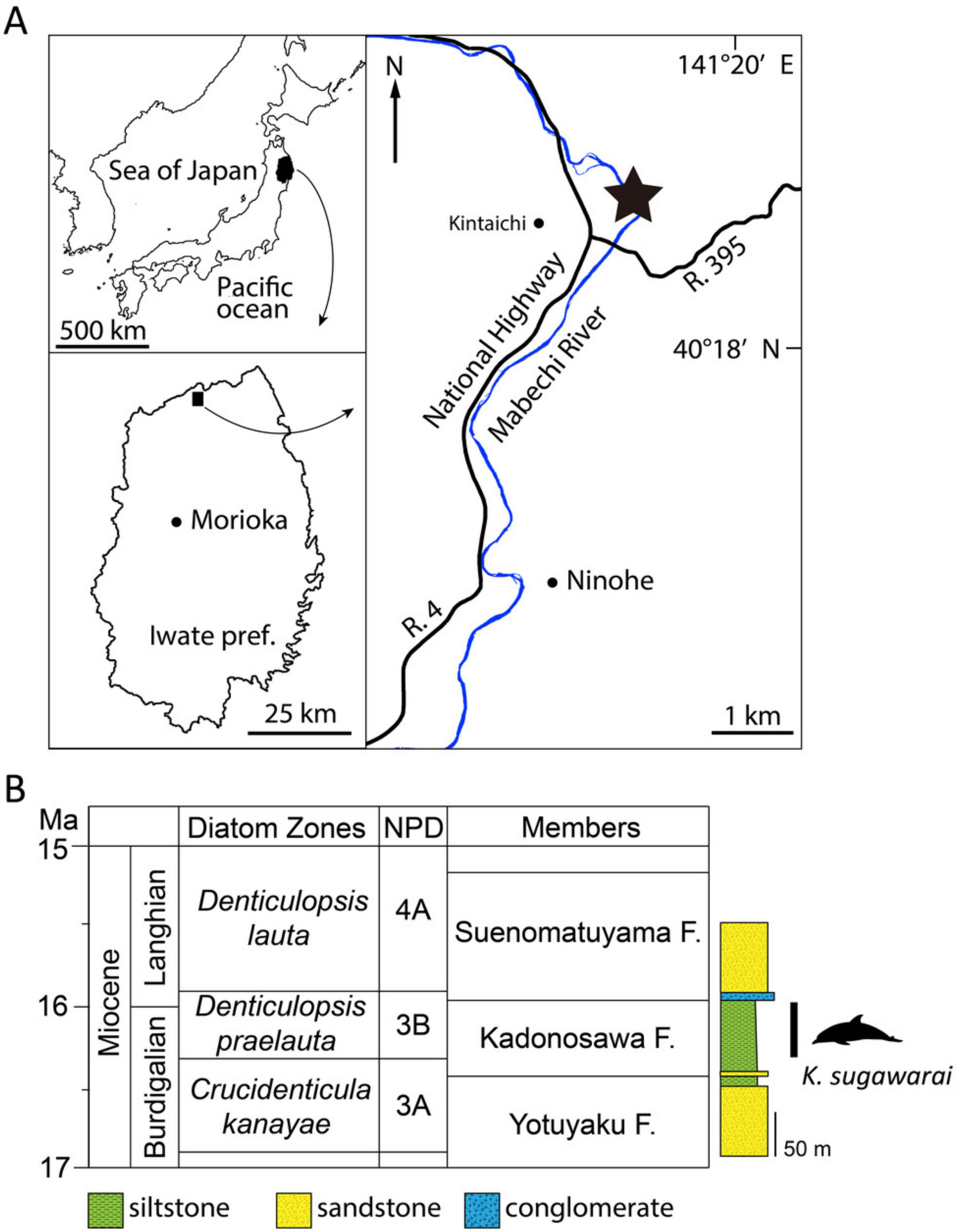
A
Sea of Japan
Pacific ocean
500 km
Morioka
Iwate pref.
25 km
N
141°20′ E
Kintaichi
National Highway
Mabechi River
R. 395
40°18′ N
Ninohe
R. 4
1 km
B
Ma
Diatom Zones
NPD
Members
15
16
17
Miocene
Langhian
Burdigalian
Denticulopsis lauta
4A
Suenomatuyama F.
Denticulopsis praelauta
3B
Kadonosawa F.
Crucidenticula kanayae
3A
Yotuyaku F.
K. sugawarai
50 m
siltstone
sandstone
conglomerate

Figure 2

Dorsal views of the skull of *Kentriodon sugawarai,* sp. nov., holotype, NHFM-F 001.

(A) photo. (B) corresponding line drawing with anatomical interpretations. Scale bar equals 100 mm.

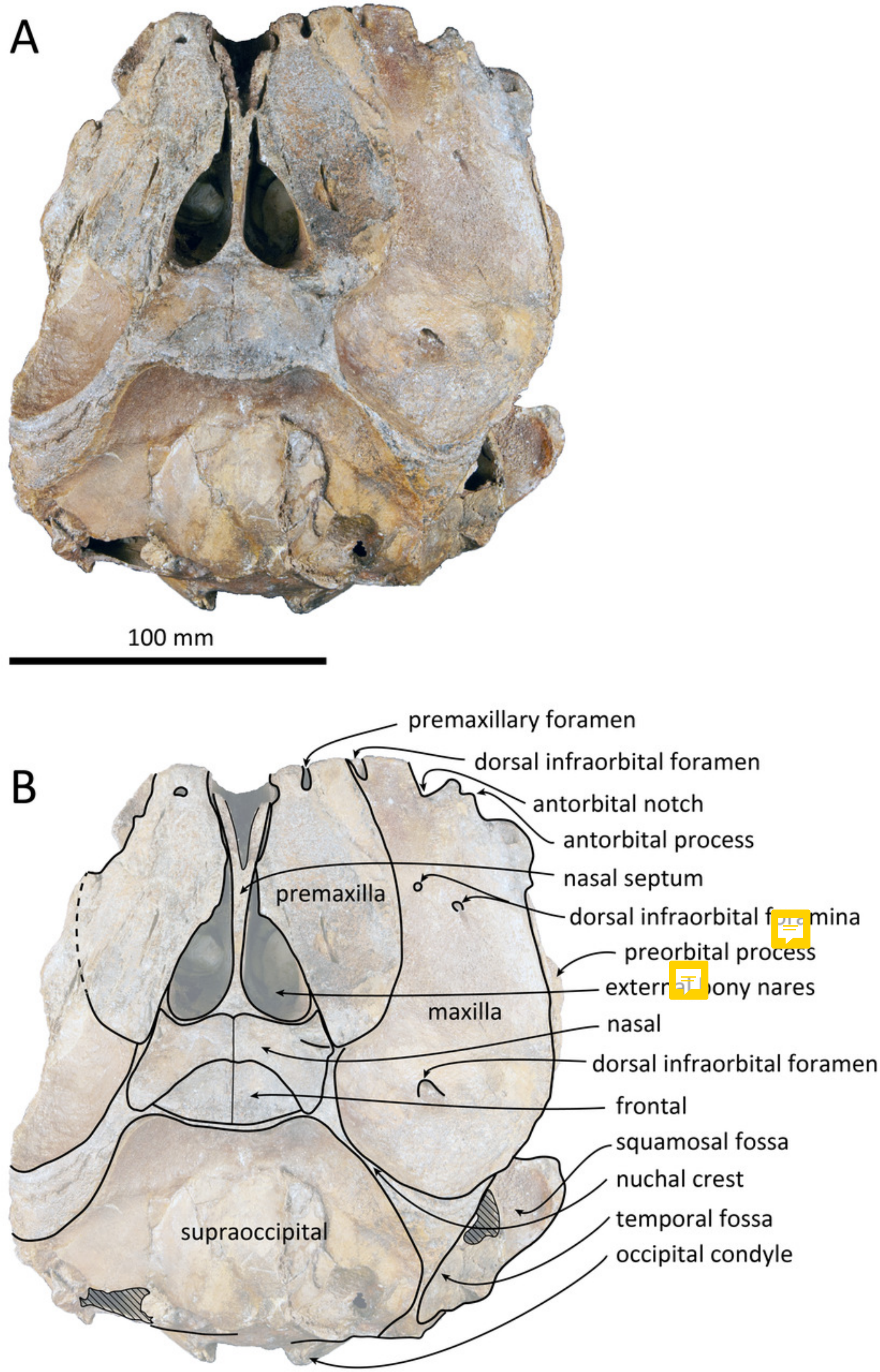
A
100 mm
B
premaxillary foramen
dorsal infraorbital foramen
antorbital notch
antorbital process
nasal septum
dorsal infraorbital foramina
preorbital process
external bony nares
nasal
dorsal infraorbital foramen
frontal
squamosal fossa
nuchal crest
temporal fossa
occipital condyle
premaxilla
maxilla
supraoccipital

Figure 3

Ventral views of the skull of *Kentriodon sugawarai,* sp. nov., holotype, NHFM-F 001.

(A) photo. (B) corresponding line drawing with anatomical interpretations. Scale bar equals 100 mm.

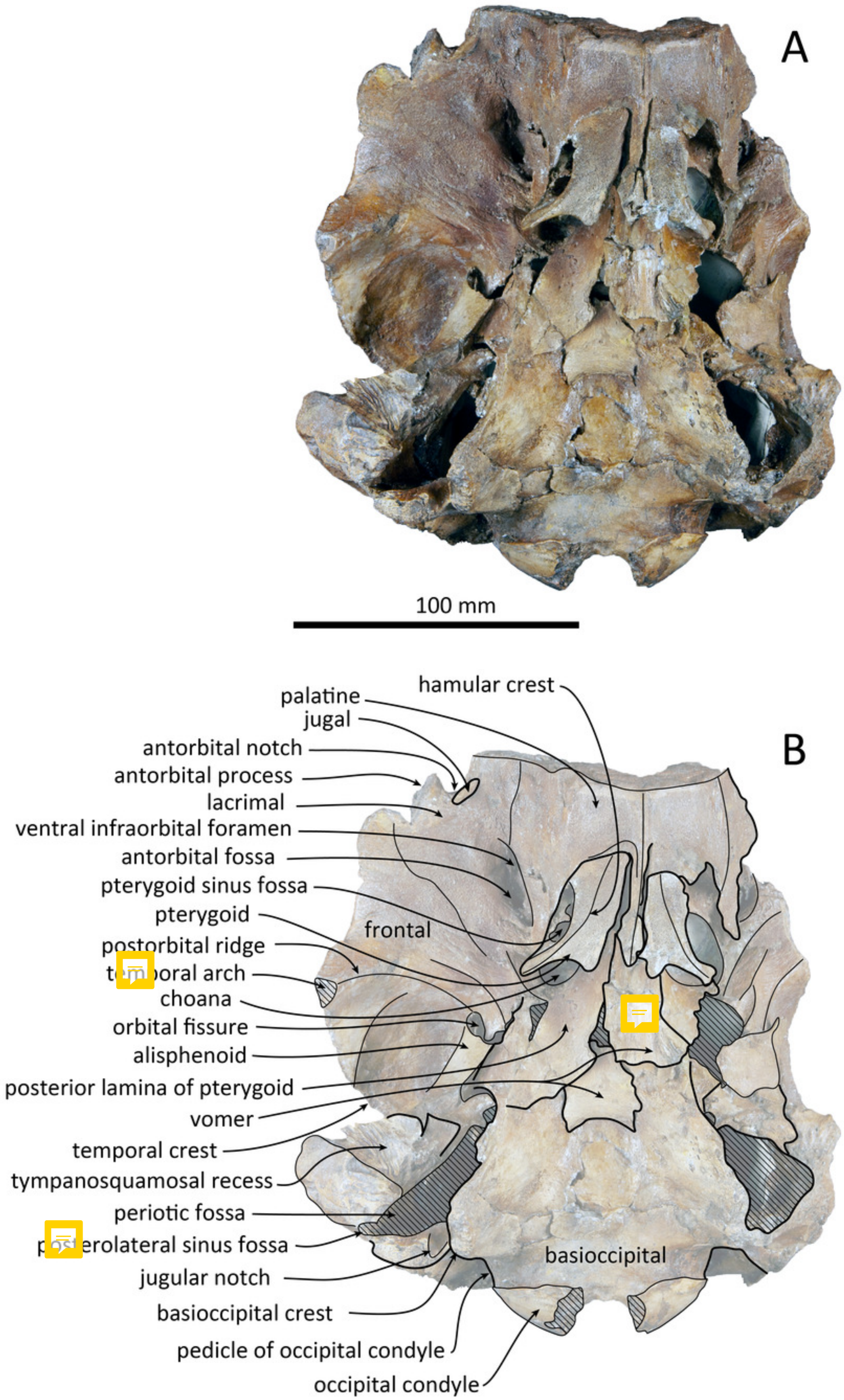
A
100 mm
B
hamular crest
palatine
jugal
antorbital notch
antorbital process
lacrimal
ventral infraorbital foramen
antorbital fossa
pterygoid sinus fossa
pterygoid
postorbital ridge
temporal arch
choana
orbital fissure
alisphenoid
posterior lamina of pterygoid
vomer
temporal crest
tympanosquamosal recess
periotic fossa
posterolateral sinus fossa
jugular notch
basioccipital crest
pedicle of occipital condyle
occipital condyle
frontal
basioccipital

Figure 4

Right lateral views of the skull of *Kentriodon sugawarai,* sp. nov., holotype, NHFM-F 001.

(A) photo. (B) corresponding line drawing with anatomical interpretations. Scale bar equals 100 mm.

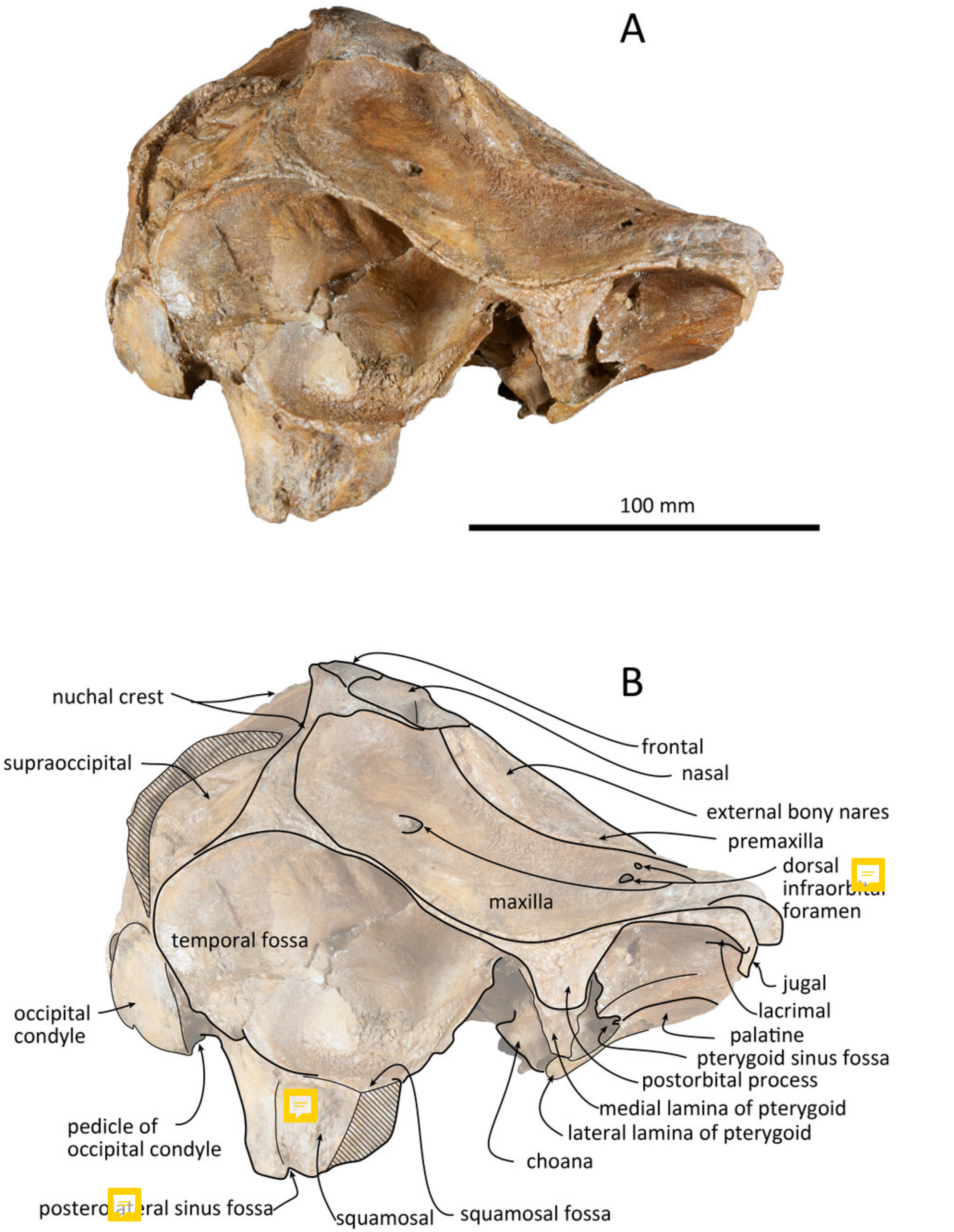
A
100 mm
B
nuchal crest
supraoccipital
frontal
nasal
external bony nares
premaxilla
dorsal
infraorbital
foramen
maxilla
temporal fossa
jugal
lacrimal
palatine
pterygoid sinus fossa
postorbital process
occipital
condyle
medial lamina of pterygoid
lateral lamina of pterygoid
pedicle of
occipital condyle
choana
posterolateral sinus fossa
squamosal
squamosal fossa

Figure 5

Anterior views of the skull of *Kentriodon sugawarai,* sp. nov., holotype, NHFM-F 001.

(A) photo. (B) corresponding line drawing with anatomical interpretations. Scale bar equals 100 mm.


A
100 mm

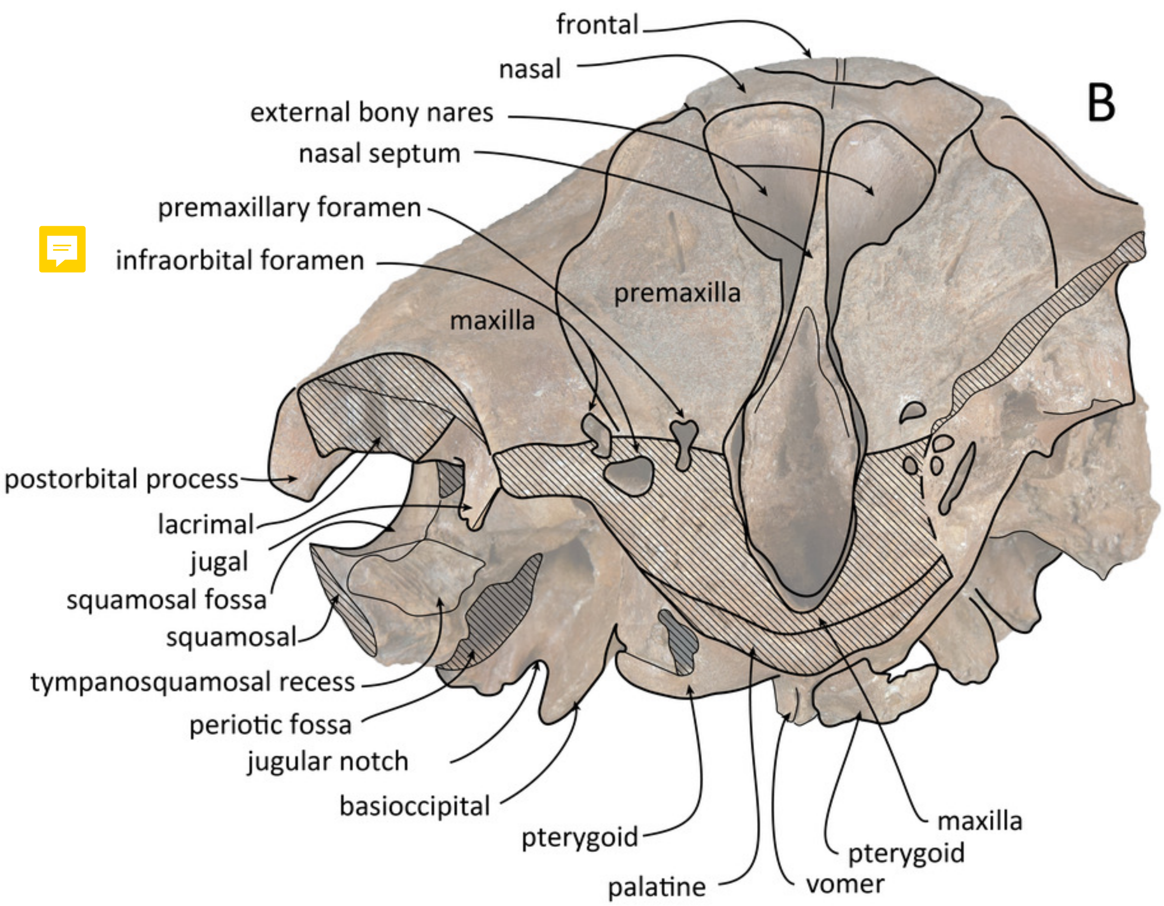
B
frontal
nasal
external bony nares
nasal septum
premaxillary foramen
infraorbital foramen
premaxilla
maxilla
postorbital process
lacrimal
jugal
squamosal fossa
squamosal
tympanosquamosal recess
periotic fossa
jugular notch
basioccipital
pterygoid
palatine
vomer
pterygoid
maxilla

Figure 6

Posterior views of the skull of *Kentriodon sugawarai,* sp. nov., holotype, NHFM-F 001.

(A) photo. (B) corresponding line drawing with anatomical interpretations. Scale bar equals 100 mm.

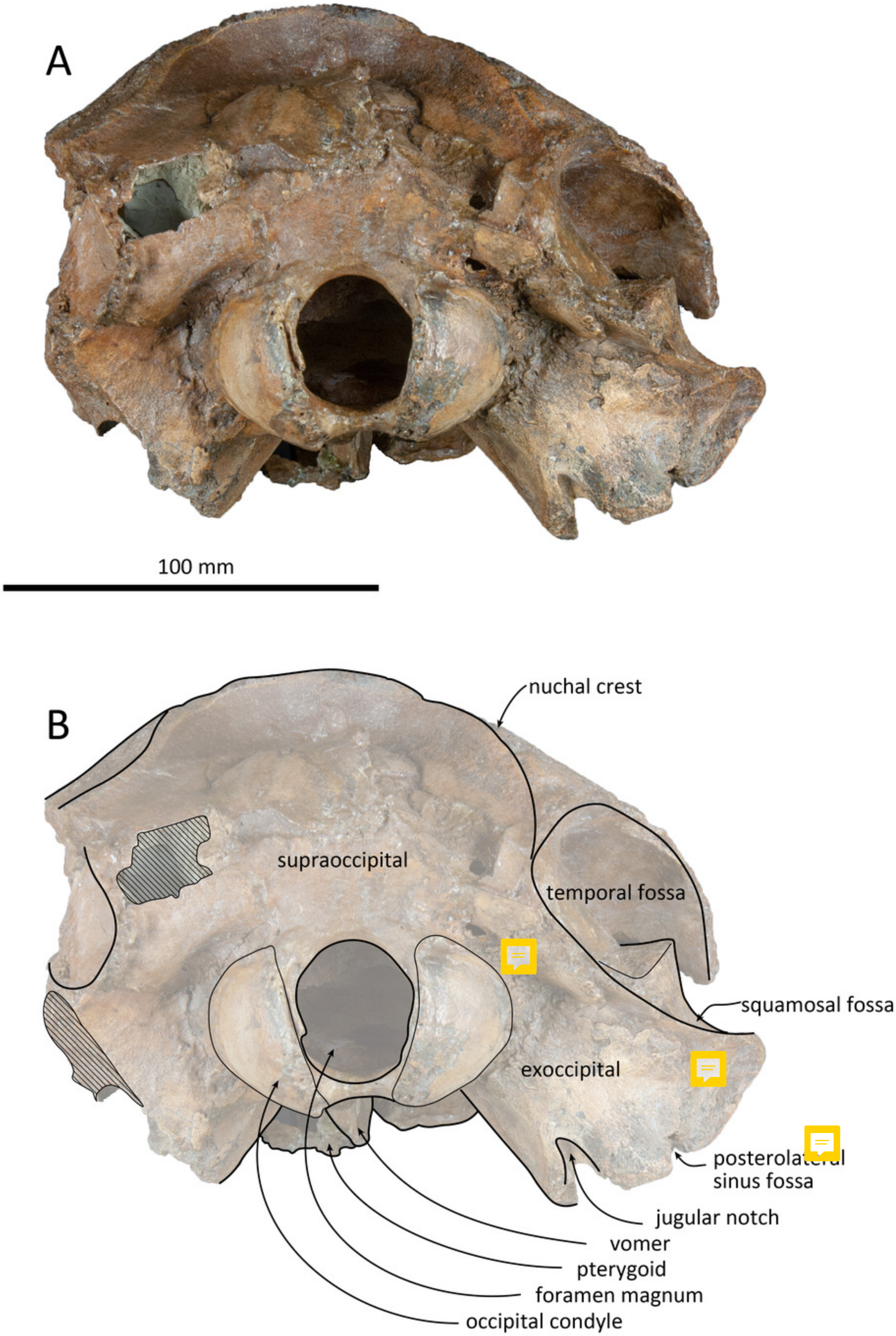
A
100 mm
B
nuchal crest
supraoccipital
temporal fossa
squamosal fossa
exoccipital
posterolateral sinus fossa
jugular notch
vomer
pterygoid
foramen magnum
occipital condyle

Figure 7

Right periotic of *Kentriodon sugawarai,* sp. nov., holotype, NHFM-F 001. (A) ventral view. (B) dorsal view. (C) medial view. (D) lateral view. (E) anterior view. (F) posterior view. Scale bar equals 20 mm.

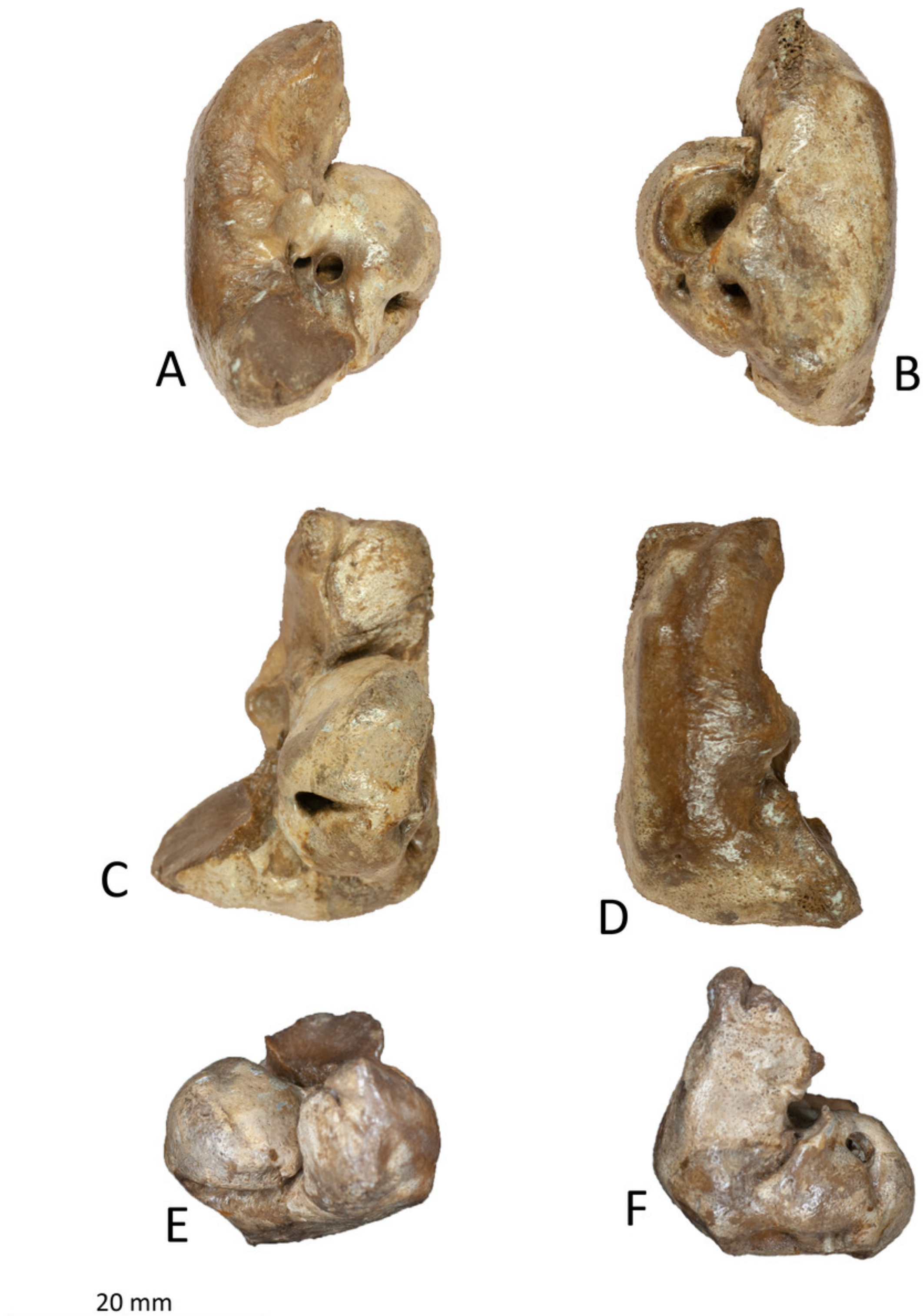
A
B
C
D
E
F
20 mm

Figure 8

Line drawings of the right periotic of *Kentriodon sugawarai,* sp. nov., holotype, NHFM-F 001, with anatomical interpretations.

(A) ventral view. (B) dorsal view. (C) medial view. (D) lateral view. (E) anterior view. (F) posterior view. Scale bar equals 20 mm.

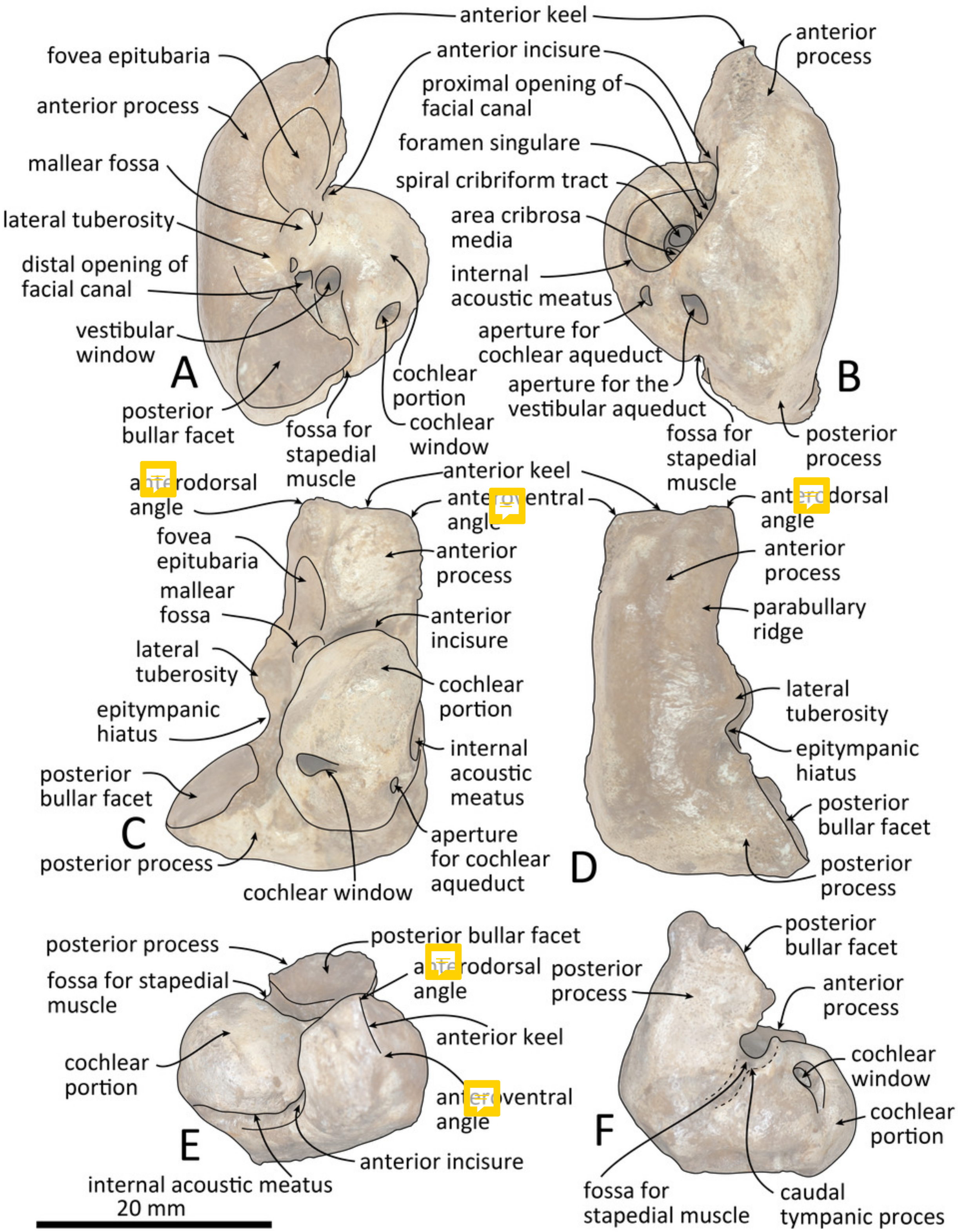
anterior keel
fovea epitubaria
anterior incisure
anterior process
proximal opening of facial canal
mallear fossa
foramen singulare
spiral cribriform tract
lateral tuberosity
area cribrosa media
distal opening of facial canal
internal acoustic meatus
vestibular window
aperture for cochlear aqueduct
A
cochlear portion
aperture for the vestibular aqueduct
B
posterior bullar facet
fossa for stapedial muscle
cochlear window
fossa for stapedial muscle
posterior process
anterodorsal angle
anteroventral angle
anterior keel
anterodorsal angle
fovea epitubaria
anterior process
anterior process
mallear fossa
parabullary ridge
anterior incisure
lateral tuberosity
cochlear portion
lateral tuberosity
epitympanic hiatus
internal acoustic meatus
epitympanic hiatus
posterior bullar facet
posterior bullar facet
C
aperture for cochlear aqueduct
posterior process
posterior process
D
cochlear window
posterior process
posterior bullar facet
posterior bullar facet
fossa for stapedial muscle
anterodorsal angle
posterior process
anterior process
anterior keel
cochlear portion
cochlear window
anteroventral angle
cochlear portion
E
F
anterior incisure
internal acoustic meatus
fossa for stapedial muscle
caudal tympanic proces
20 mm

Figure 9

Right tympanic bulla of *Kentriodon sugawarai,* sp. nov., hototype, NHFM-F 001.

(A) dorsal view of the posterior process of the tympanic bulla. (B–C) ~~accesorry~~ ossicle. (B) dorsal view. (C) ventral view. (D–I), left tympanic bulla. (D) dorsal view. (E) ventral view. (F) lateral view. (G) medial view. (H) anterior view. (I) posterior view. Scale bar equals 20 mm.

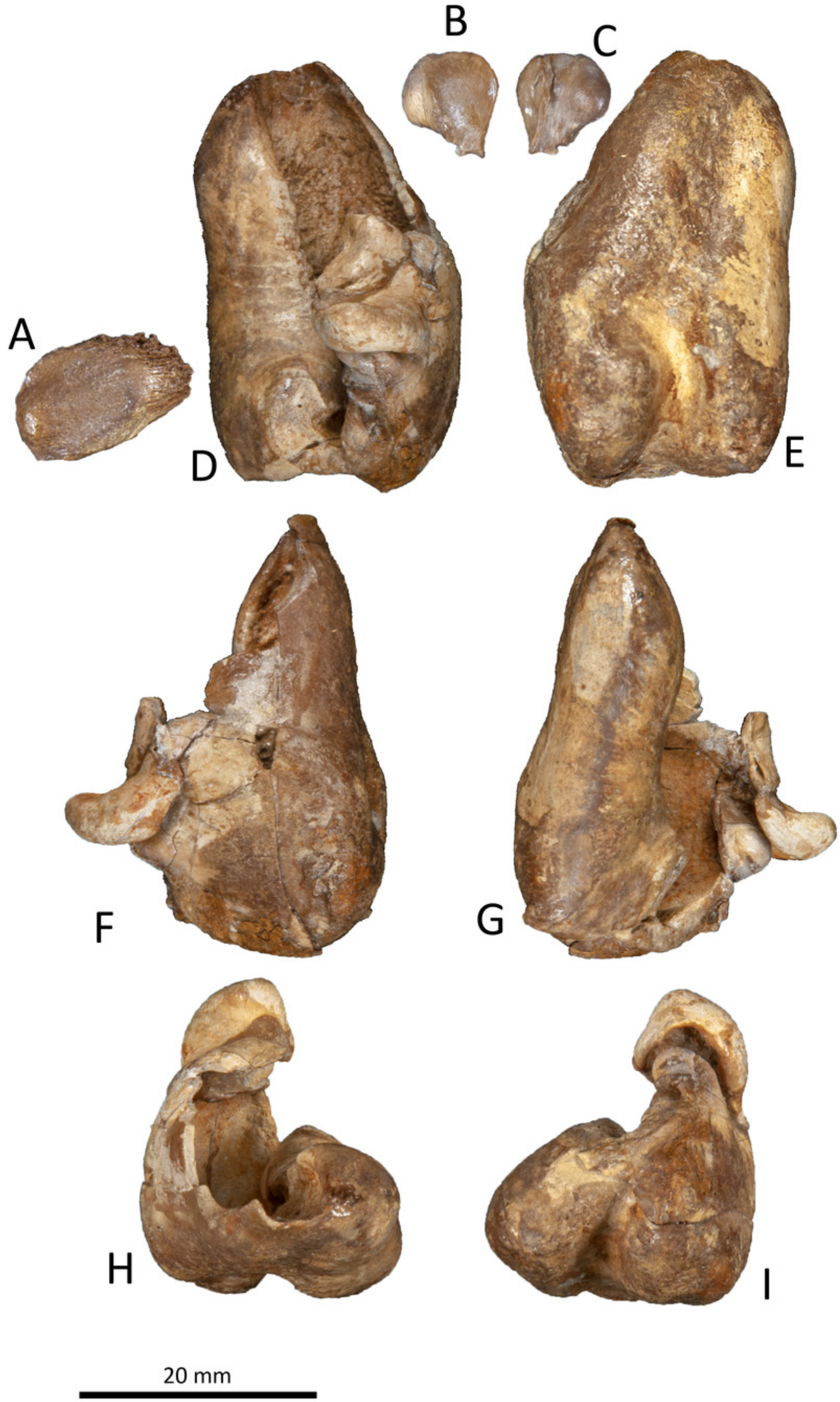
A
B
C
D
E
F
G
H
I
20 mm

Figure 10

Line drawings of the right tympanic bulla of *Kentriodon sugawarai,* sp. nov., holotypes, NHFM-F 001.

(A) dorsal view of the posterior process of the tympanic bulla. (B–C) accesorry ossicle. (B) dorsal view. (C) ventral view. (D–I) left tympanic bulla. (D) dorsal view. (E) ventral view. (F) lateral view. (G) medial view. (H) anterior view. (I) posterior view. Scale bar equals 20 mm.

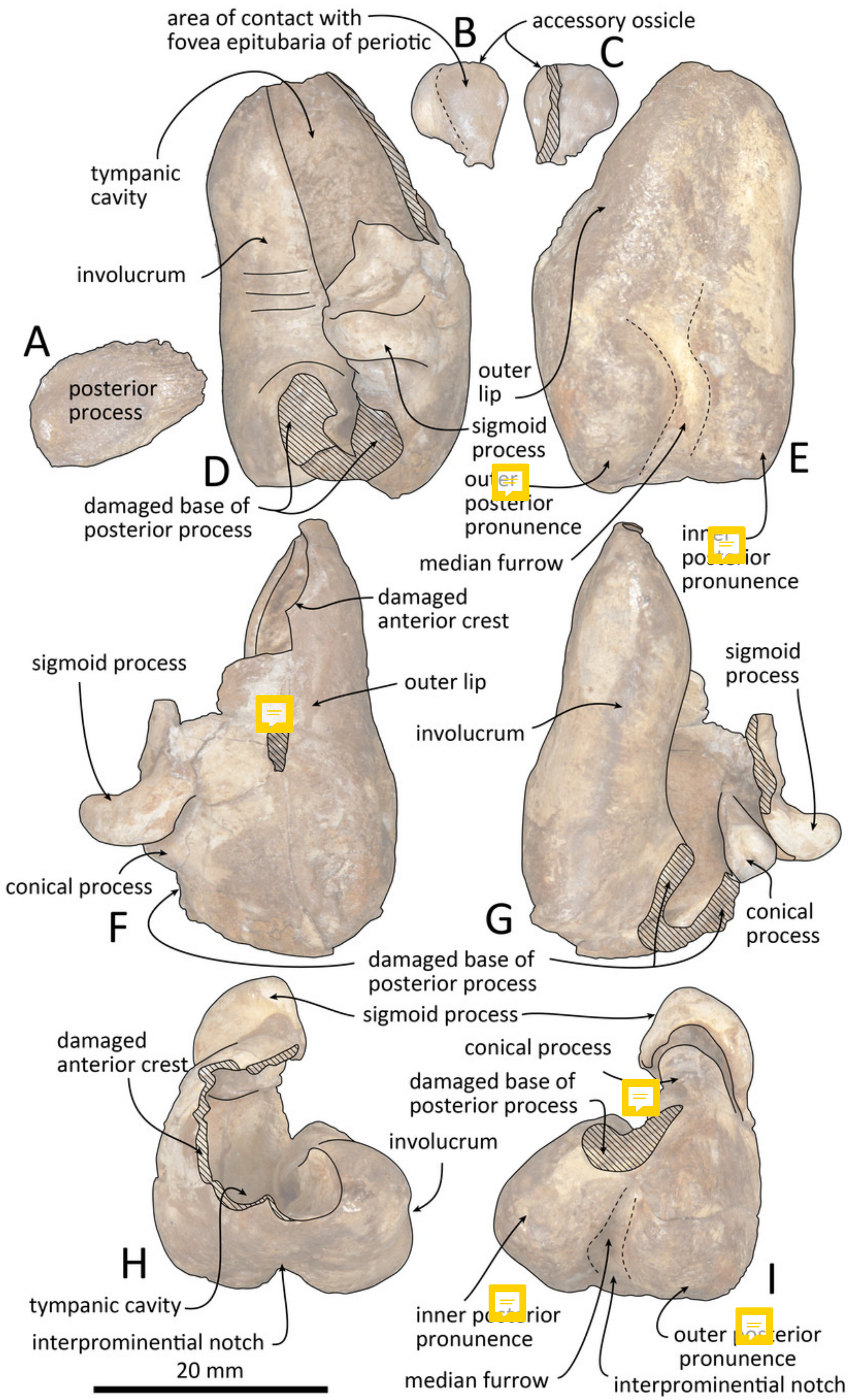
area of contact with
fovea epitubaria of periotic
B
accessory ossicle
C
tympanic
cavity
involucrum
A
posterior
process
outer
lip
sigmoid
process
D
E
damaged base of
posterior process
posterior
pronunence
median furrow
pronunence
damaged
anterior crest
sigmoid process
outer lip
sigmoid
process
involucrum
conical process
F
G
conical
process
damaged base of
posterior process
sigmoid process
damaged
anterior crest
conical process
damaged base of
posterior process
involucrum
H
I
tympanic cavity
interprominential notch
inner
pronunence
outer
pronunence
median furrow
interprominential notch
20 mm

Figure 11

~~Middle ear ossicle~~, tooth, mandible and vertebra of *Kentriodon sugawarai,* sp. nov., holotypes, NHFM-F 001, with anatomical interpretations.

(A–F) right malleus. (A) ventral view. (B) dorsal view. (C) medial view. (D) lateral view. (E) anterior view. (F) posterior view. (G–J) probable upper tooth. (G) distal view. (H) mesial view. (I) lingual view. (J) labial view. (K–L) ascending ramus of the left mandible. (K) lingual view. (L) labial view. (M–N) horizontal ramus of the right mandible. (M) lingual view. (N) labial view. (O–P) ventral half of the atlas. (O) cranial view. (P) caudal view. Scale bar equals 20 mm.

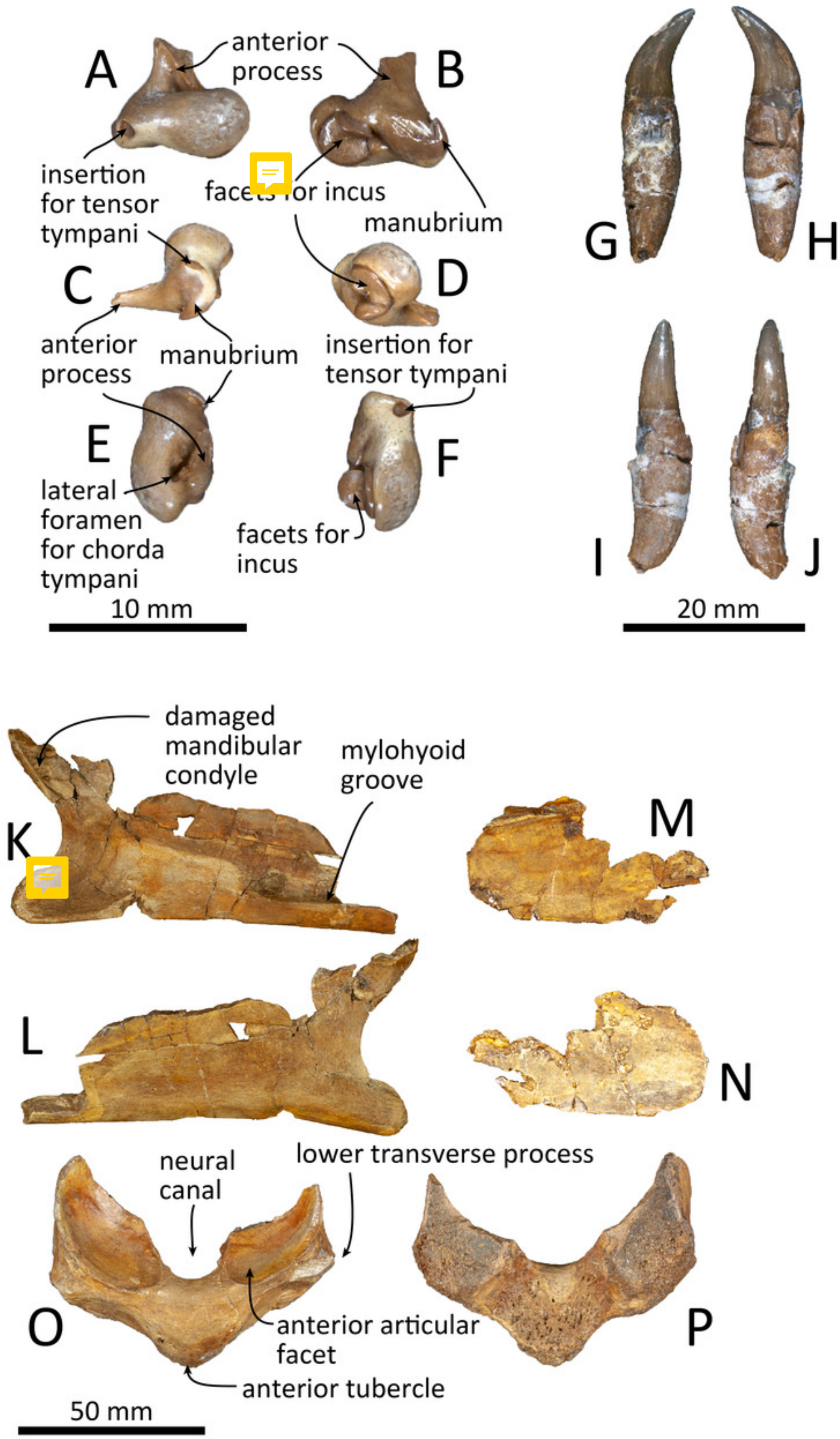
A
anterior
process
B
insertion
for tensor
tympani
manubrium
C
D
anterior
process
manubrium
insertion for
tensor tympani
E
F
lateral
foramen
for chorda
tympani
facets for
incus
10 mm
G
H
I
J
20 mm
damaged
mandibular
condyle
mylohyoid
groove
K
M
L
N
neural
canal
lower transverse process
anterior articular
facet
anterior tubercle
O
P
50 mm

Figure 12

Phylogenetic relationships of *Kentriodon sugawarai*, sp. nov.

50% majority consensus tree resulting from 256 most parsimonious trees with tree constraint by the molecular “consensus” tree from McGowen, Spaulding & Gatesy (2009), McGowen et al. (2011) and McGowen et al. (2020), 3424 steps long, with the consistency index = 0.197 and the retention index = 0.564. Numbers below nodes indicate bootstrap values (1,000 replicate~~d~~). The values ~~less~~ than 50% were omitted. The interspecific relationships ~~of~~ clades Physeteroidea, Ziphiidae, Delphinidae, Phocoenidae and Monodontidae were omitted and represented by superfamilial and familial ranks.

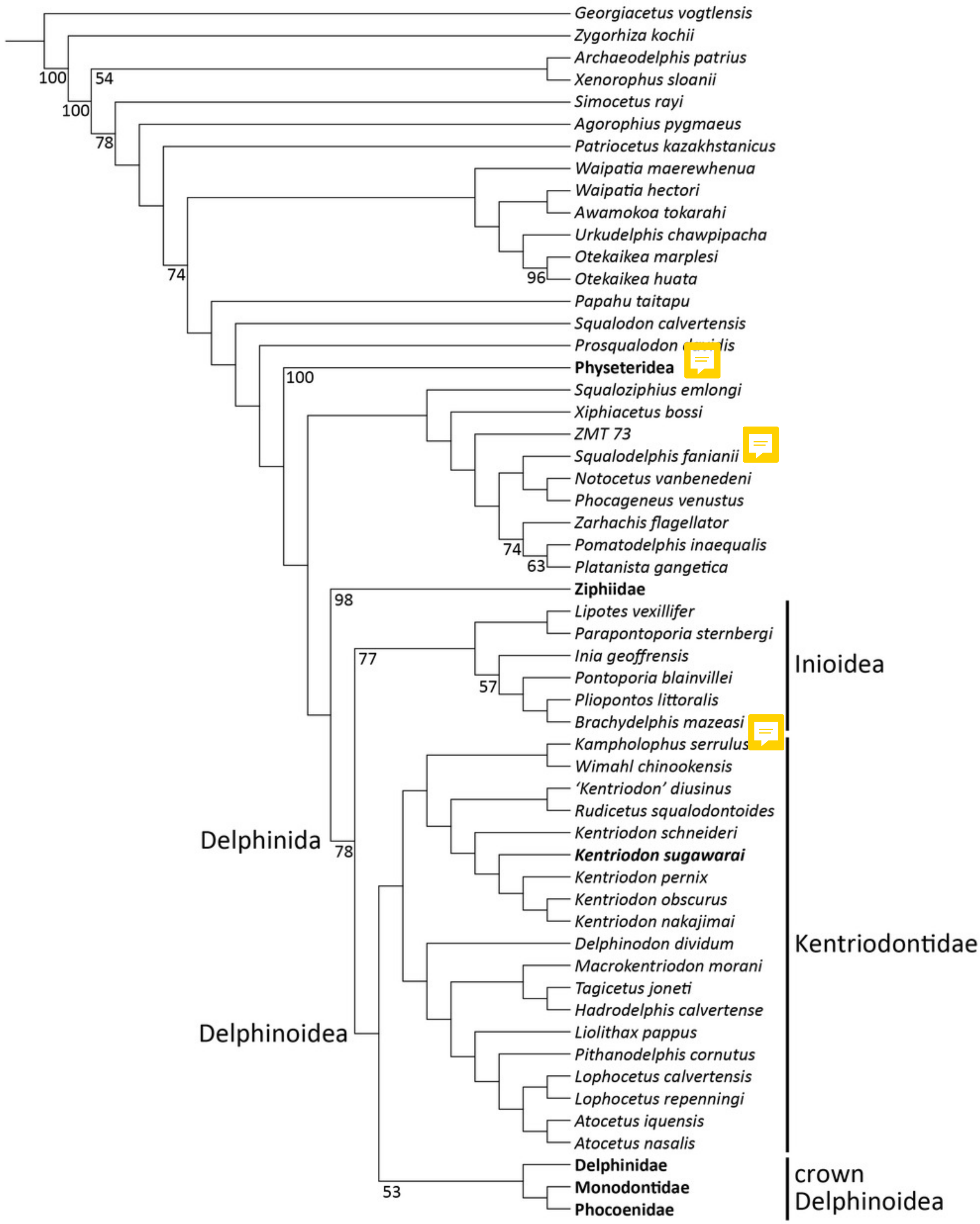
Georgiacetus vogtlensis
Zygorhiza kochii
Archaeodelphis patrius
Xenorophus sloanii
Simocetus rayi
Agorophius pygmaeus
Patriocetus kazakhstanicus
Waipatia maerewhenua
Waipatia hectori
Awamokoa tokarahi
Urkudelphis chawpipacha
Otekaikea marplesi
Otekaikea huata
Papahu taitapu
Squalodon calvertensis
Prosqualodon
Physeteridea
Squaloziphius emlongi
Xiphiacetus bossi
ZMT 73
Squalodelphis fanianii
Notocetus vanbenedeni
Phocageneus venustus
Zarhachis flagellator
Pomatodelphis inaequalis
Platanista gangetica
Ziphiidae
Lipotes vexillifer
Parapontoporia sternbergi
Inia geoffrensis
Pontoporia blainvillei
Pliopontos littoralis
Brachydelphis mazeasi
Kampholophus serrulus
Wimahl chinookensis
'Kentriodon' diusinus
Rudicetus squalodontoides
Kentriodon schneideri
Kentriodon sugawarai
Kentriodon pernix
Kentriodon obscurus
Kentriodon nakajimai
Delphinodon dividum
Macrokentriodon morani
Tagicetus joneti
Hadrodelphis calvertense
Liolithax pappus
Pithanodelphis cornutus
Lophocetus calvertensis
Lophocetus repenningi
Atocetus iquensis
Atocetus nasalis
Delphinidae
Monodontidae
Phocoenidae
Inioidea
Kentriodontidae
crown Delphinoidea
Delphinida
Delphinoidea
100
54
100
78
74
96
100
74
63
98
77
57
78
53

Table 1(on next page)

Measurements (in mm) for the skull and tympanoperiotic of *Kentriodon sugawarai* sp. nov., holotype, NHFM–F 001.

Abbreviations: e, estimate; +, not complete.

Dimension	Measurement
Skull	
Condylobasal length - from tip of rostrum to hindmost margin of occipital condyles.	186.2+
Length of rostrum - from tip to line across hindmost limits of antorbital notches.	15.1+
Width of rostrum at base - along line across hindmost limits of antorbital notches.	107.2e
Maximum length of frontal at the vertex	19.3
Width of the foramen magnum	21.8
Width of premaxillae at posterior extremity	61.4
Width of nasal bones	53.4
Distance from tip of rostrum to external nares (to mesial end of anterior ~~transverse~~ margin of right naris).	56.0+
Distance from tip of rostrum to internal nares (to mesial end of posterior margin of right pterygoid).	56.8+
Greatest preorbital width.	181.2e
Greatest postorbital width.	215.0e
Least supraorbital width.	179.2e
Greatest width of external nares.	41.8
Greatest width across zygomatic processes of squamosal.	161.0+
Greatest width of ~~premaxillaries.~~	101.4e
Greatest parietal width.	138.0+
Greatest length of left posttemporal fossa, measured to external margin of raised suture.	110
Greatest width of left posttemporal fossa ~~at right angles~~ to greatest length.	54.5
Major diameter of left temporal fossa proper.	41.6
Minor diameter of left temporal fossa proper.	48.1+
Distance from foremost end of junction between nasals to hindmost point of margin of supraoccipital crest.	34.6
Length of left orbit-from apex of preorbital process of frontal to apex of postorbital process.	52.4
Length of antorbital process of left lacrimal.	18+
Greatest width of internal nares.	71.4e
Greatest length of left pterygoid.	47.6
Width across occipital condyles	70.5
Width of atlas	69.1
Length of atlas	62.9+
Periotic	
Total length	31.7
Length of anterior process	17.8
Width at pars cochlearis	13.2
Length of posterior bullar facet	10.5
Width of posterior bullar facet	9.9
Length of pars cochlearis	17.2
Tympanic Bulla	

Total length as preserved	37.4
Total width as preserved	21.8
Width of inner posterior prominence	9.5